4.5 H_2L4 and its Ni(II), Cu(II) and Zn(II) complexes

4.5.1 H_2L4

H_2L4 was obtained as a dark grey powder in good yield (76%) from the reaction shown in **Scheme 4.1** (X = 3-OH). The results from the CHN elemental analysis are in excellent agreement with the chemical formula, $C_{23}H_{17}O_4N_5$.

The **FTIR** spectrum (**Figure 4.47)** shows the characteristics broad peak at 3446 cm^{-1} for intra-molecularly hydrogen bonded -OH group [1], a strong peak due to C=N stretching at 1627 cm^{-1}, another strong peak at 1255 cm^{-1} assigned to C-O phenolic stretching, and peaks in the region 1000 - 1500 cm^{-1} from benzene ring skeletal vibrations. The peak at 779 cm^{-1} is due to aromatic C-H out-of-plane stretching mode. The result strongly supports the formation of the Schiff base [81].

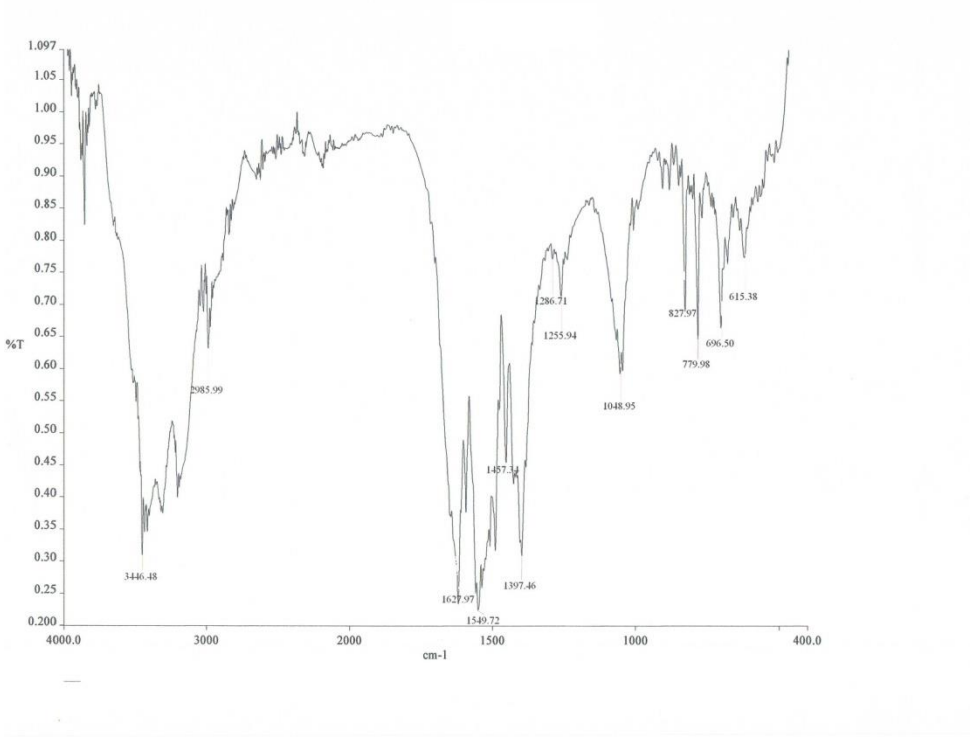

Figure 4.47 FTIR spectrum of H_2L4

The **^{1}H-NMR** spectrum (**Figure 4.48) is** consistent with the expected structural formula of H_2L4: a singlet at 10.16ppm is due to phenolic hydrogen; a singlet at 8.21 ppm is due to imino hydrogen; and a multiplet in the range 6.70 - 7.61 ppm is due to the aromatic hydrogens. The integration ratio for these hydrogens is 2:1:5.5 respectively (expected ratio =2:1:5.5), and supports the molecular symmetry for the Schiff base [68].

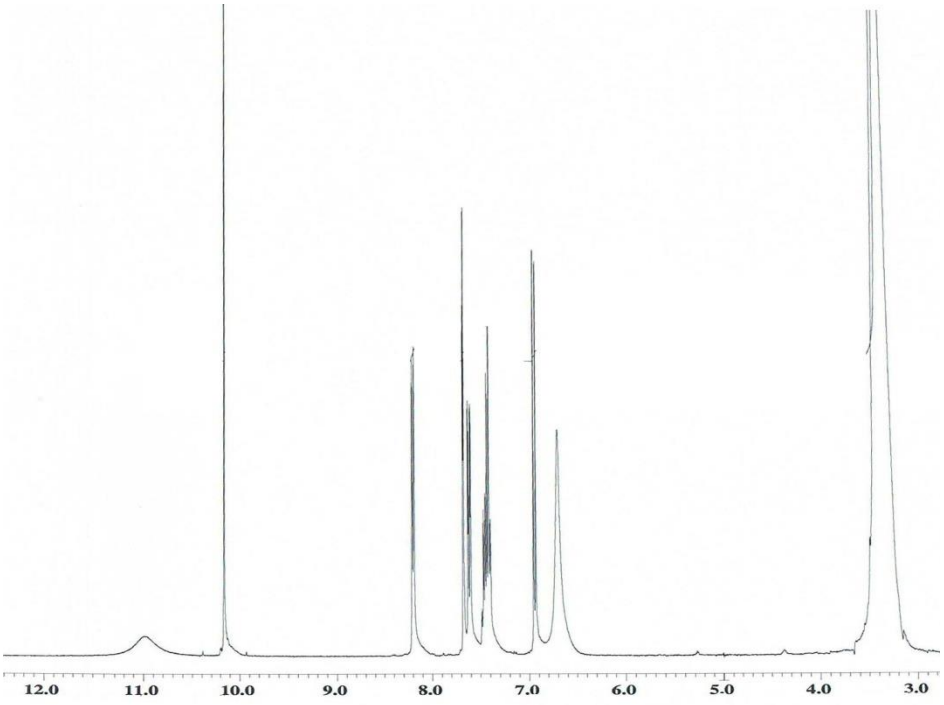

Figure 4.48 ^{1}H-NMR spectrum of H_2L4

The **^{13}C-NMR** spectrum (**Figure 4.49**) shows 12 peaks, assigned as follows: 120.4, 124.5, 137.5 and 139 ppm phenol, 128.1, 128.6, 131.0, 131.5 phenyl ring, 170.6 triazine ring, and 160.3 C=N. Other peaks are overlapping.

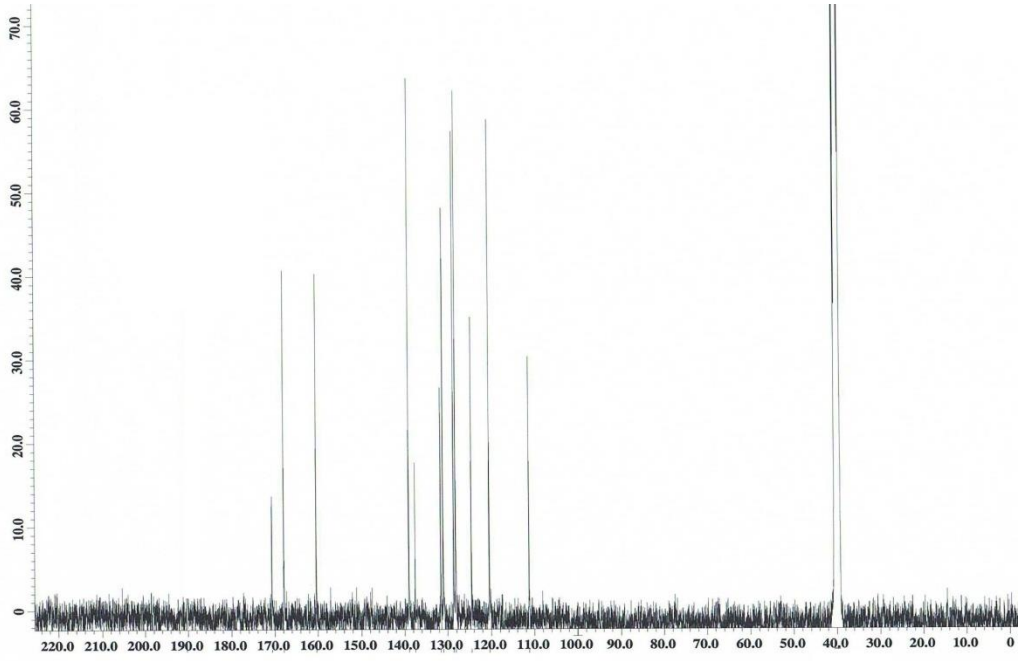

Figure 4.49 ^{13}C-NMR spectrum of H_2L4

The **UV-vis** spectrum of a solution of H_2L4 in DMSO (**Figure 4.50** shows a high intensity broaden absorption band at about 286 nm ($\varepsilon = 1.4x10^4$ $M^{-1}cm^{-1}$) assigned to π-π^* transition of the aromatic ring. The *n*-π^* transition of the azomethine chromophore is observed as a shoulder at the high intensity peak at about 344 nm ($\varepsilon = 1.2x10^4$ $M^{-1}cm^{-1}$). These values are in agreement with other Schiff bases reported in the literature [80].

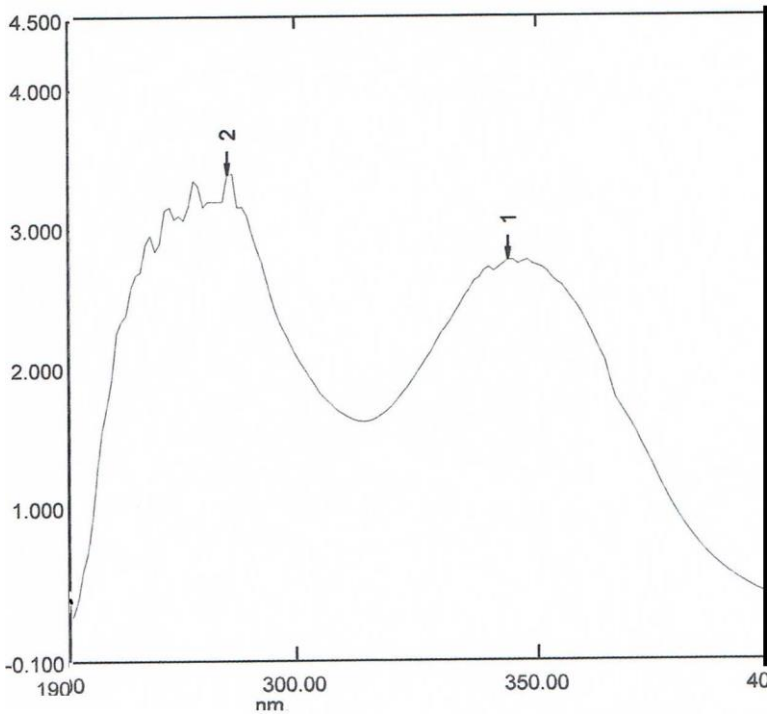

Figure 4.50 UV-vis spectrum of H_2L4 in DMSO

4.5.2 Nickel(II) complex of H_2L4

The nickel(II) complex (NiL4) was obtained as a dark brown powder in good yield (72%) in the reaction between H_2L4 and nickel(II) acetate tetrahydrate in presence of triethylamine.

The results from the **CHN** elemental analyses are in excellent agreement with the chemical formula, $[Ni(C_{23}H_{15}O_4N_5)(H_2O)_2]$ or $[NiL4(H_2O)_2]$.

The **FTIR** spectrum (**Figure 4.51**) differs from that of H_2L4 (**Figure 4.47**). It is further noted that the -OH peak, observed for H_2L4 at 3446cm^{-1}, is now observed at 3310 cm^{-1}, and is assigned to coordinated H_2O molecules in agreement with the results from the elemental analyses .The peaks for C=N at 1627 cm^{-1} and C-O at 1255cm^{-1} observed for H_2L4 are observed at 1622 cm^{-1} and 1255 cm^{-1} respectively in NiL4. The Ni-O peak is observed at 565 cm^{-1}. These suggest that the phenolic oxygens and imino nitrogens are coordinated to Ni(II) [70].

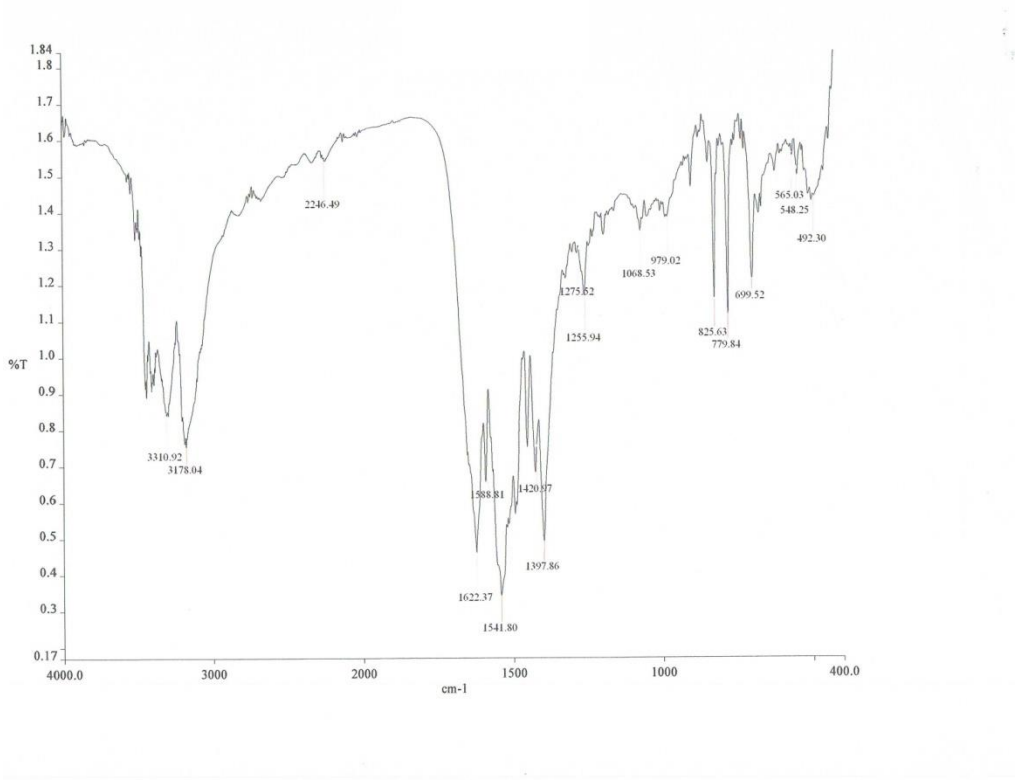

Figure 4.51 FTIR spectrum of $[NiL4(H_2O)_2]$

The **UV-vis** spectrum (**Figure 4.52;** shown as insert) shows weak *d-d* bands 902 (ε_{max} = 405 $M^{-1}cm^{-1}$), and 736 nm (ε_{max} = 189 $M^{-1}cm^{-1}$). These are consistent with an octahedral configuration at Ni(II), and using the Tanabe-Sugano diagram for d^8 complex (**Figure 4.53**), these bands are assigned to the transitions $^3A_{2g} \rightarrow {}^3T_{2g}$, $^3A_{2g} \rightarrow {}^3T_{1g}(F)$ and $^3A_{2g} \rightarrow {}^3T_{1g}(P)$, respectively, and the value of Δ_o is 13,643 cm^{-1}.

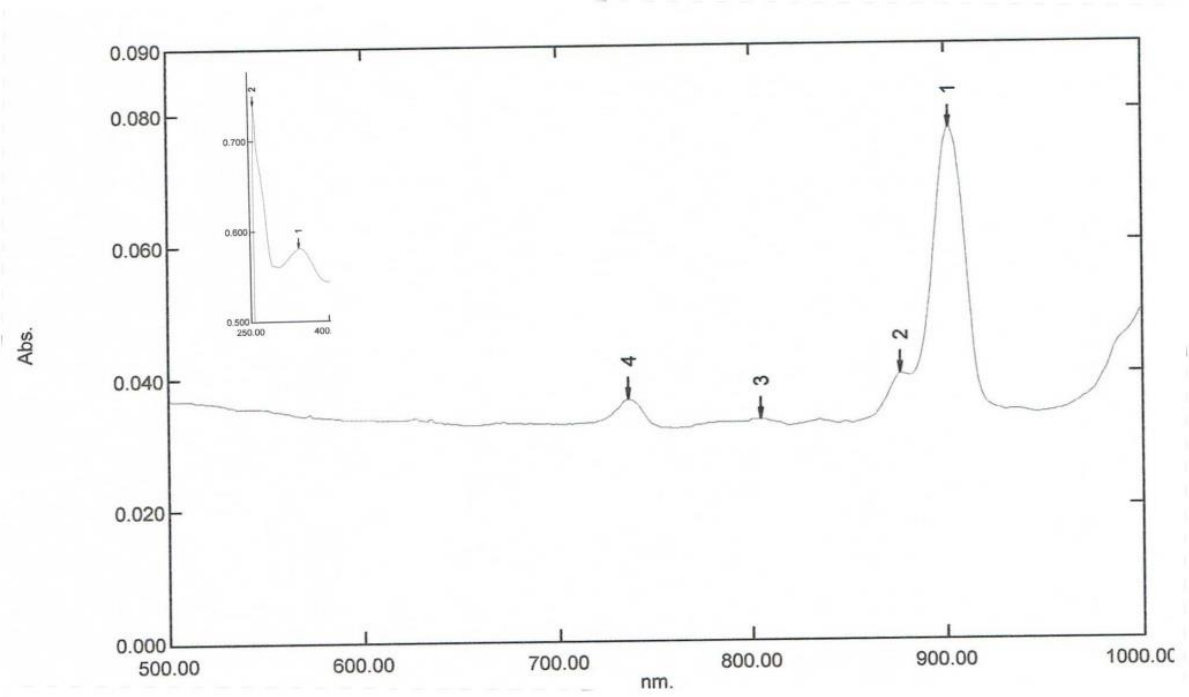

Figure 4.52 UV-vis spectrum of [NiL4$(H_2O)_2$] in DMSO

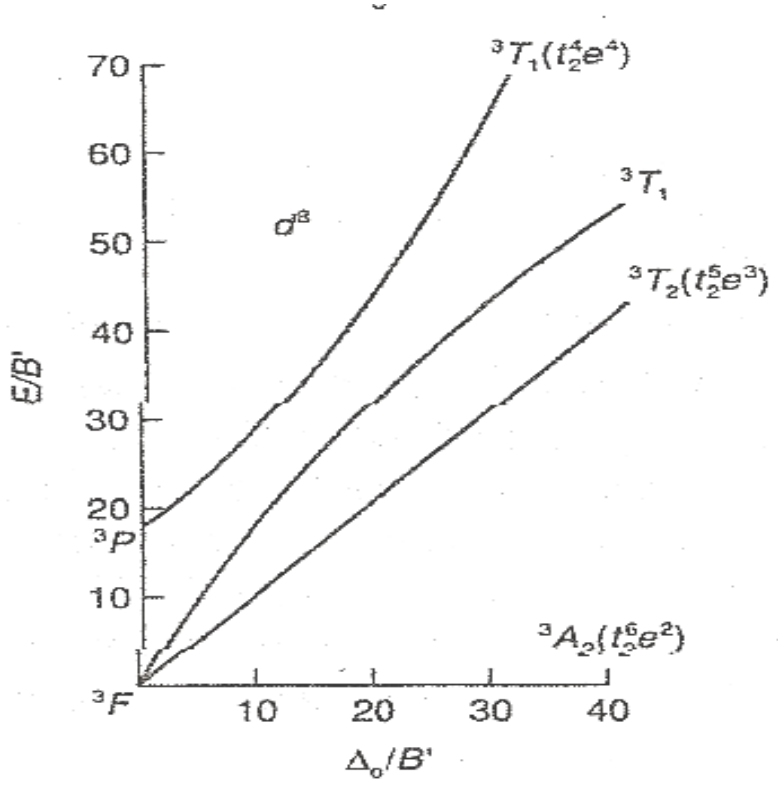

Figure 4.53 Tanabe-Sugano diagram for d^8 octahedral complexes

The peak at 343 nm ($\varepsilon = 0.31 \times 10^4$ $M^{-1}cm^{-1}$) is assigned to metal-ligand charge transfer (MLCT). The spectrum is also compared with that of H_2L4 (**Figure 4.50**). It is noted that the π - π^* band observed for H_2L4 286 nm($\varepsilon = 1.4 \times 10^4$ $M^{-1}cm^{-1}$) remains shifted in the complex 260 nm($\varepsilon = 0.38 \times 10^4$ $M^{-1}cm^{-1}$). However, the *n* - π^* band may be hidden under the strong MLCT band at 343 nm. Thus, this band is significantly red-shifted from about 300 nm to about 400 nm as a result of complexation to the Ni(II). These results are in agreement with literature result indicating the formation of the complex [82].

The **TGA** thermogram **(Figure 4.54)**, measured from 50^{o}C up to 900^{o}C, shows that the complex was stable up to 200^{o}C. The first weight loss of 2.8% at 140^{o}C corresponds to the loss of coordinated H_2O molecules (expected, 6.9%). The next step represents a total weight loss of 81.4% and is assigned to the decomposition of the ligand (expected, 82.1%). The amount of

residue at 700^{o}C is 15.8%. Assuming that the residue is Ni, the expected value is 14.3%, which is within the acceptable experimental error.

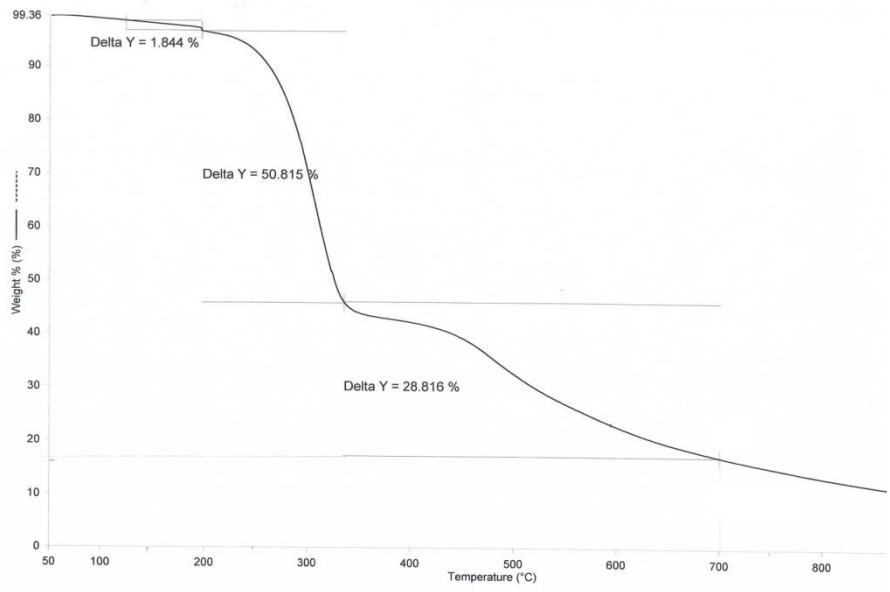

Figure 4.54TGA for [NiL4(H_2O)$_2$]

Based on the above analytical results, the proposed structure for [NiL4(H_2O)$_2$] is shown in **Figure 4.55.**

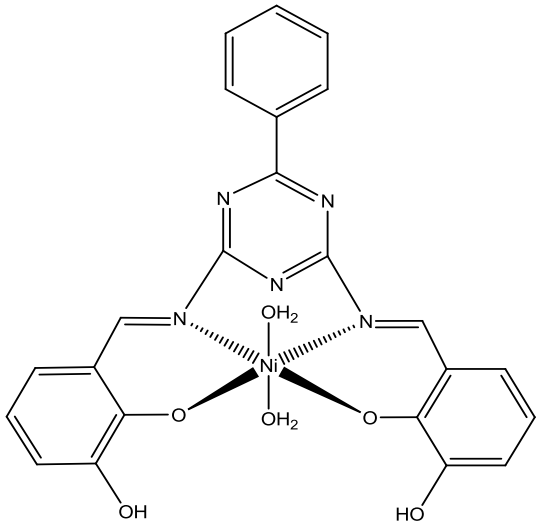

Figure 4.55 Proposed structural formula of [NiL4(H_2O)$_2$

4.5.3 Copper(II) complex of H_2L4

The copper(II) complex was obtained as a dark brown powder in good yield (73%) in the reaction between H_2L4 and copper(II) acetate monohydrate in presence of triethylamine. The yield is similar to Ni(II) complex (72%), indicating similar solubility in ethanol.

The results from the **CHN** elemental analyses are in excellent agreement with the expected chemical formula $CuC_{23}H_{15}O_4N_5$ or [CuL4 (H_2O)].

The **FTIR** spectrum (**Figure 4.56**) shows the expected functional groups as previously discussed for the corresponding Ni(II) complex (**Figure 4.51**). The C=N, C-O and Cu-O peaks for [CuL4].H_2O are at 1624 cm^{-1}, 1258 cm^{-1} and 565respectively. These are almost similar to those of the corresponding Ni(II) complex, suggesting similar bond strength.

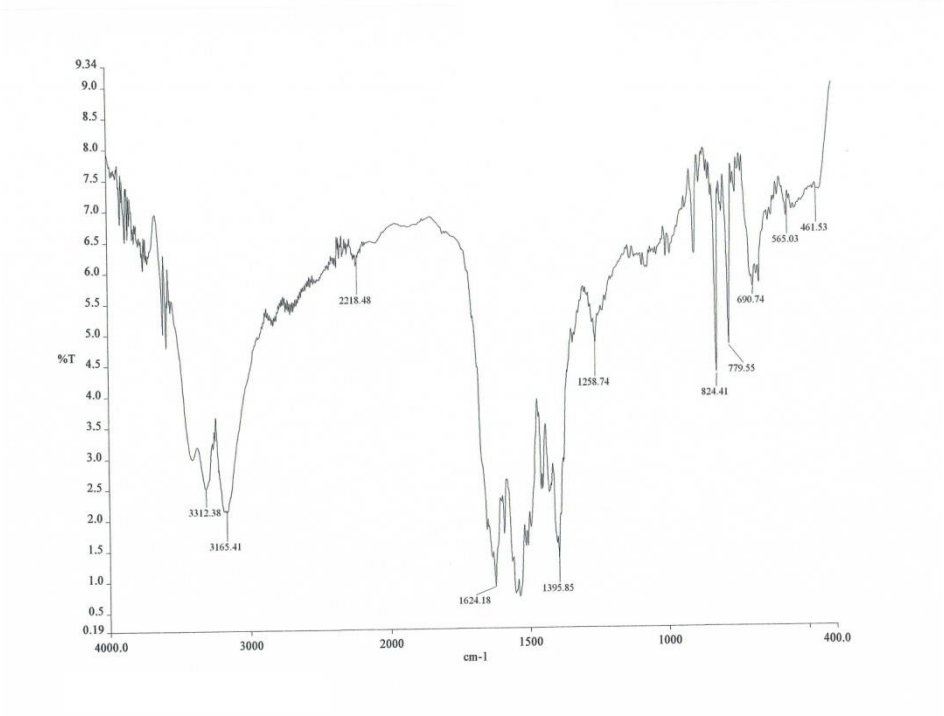

Figure 4.56 FTIR spectrum of [CuL4(H_2O)]

The **UV-vis** spectrum (**Figure 4.57**) shows a broad *d-d* peak at 690 nm (ε_{max} = 200 M^{-1} cm^{-1}). Thus, [CuL4(H_2O)] is a mononuclear square pyramidal complex [71]. The π-π^* and

MLCT bands are at 260 nm (ε_{max} = 0.4 x 10^4 $M^{-1}cm^{-1}$), and 420 nm (ε_{max} = 0.2 x 10^4 $M^{-1}cm^{-1}$) respectively, which are almost the same as for the corresponding Ni(II) complex (260 nm, 343 nm), and may be similarly explained.

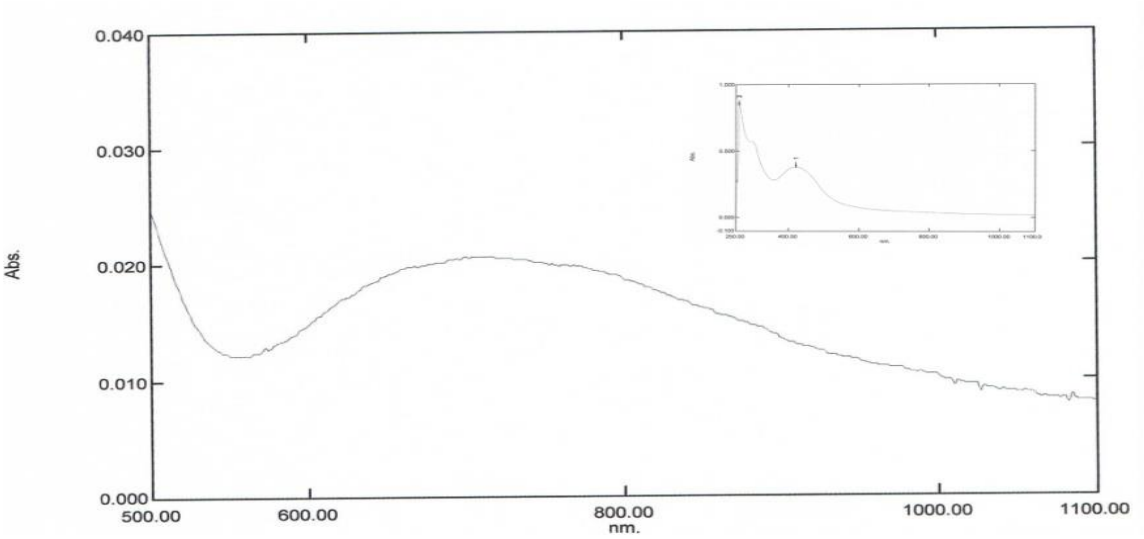

Figure 4.57 UV-vis spectrum of [CuL4(H_2O)]

The **TGA** thermogram **(Figure 4.58)**, measured from 50^oC up to 900^oC, shows that the complex was stable up to 205^oC. Thus, it is as themally stable as [NiL4(H_2O)$_2$] (200^oC).

The first weight loss of 4.6% at 150^oC corresponds to the loss of coordinated H_2O molecule (expected, 3.5%). The next step represents a total weight loss of 80.8% and is assigned to the decomposition of the ligand (expected, 84.6%). The amount of residue at about 650^oC is 14.6%. Assuming that the residue is CuO, the expected value is 15.7%. Thus, the thermal properties of [CuL4(H_2O)] is similar from that of [NiL4(H_2O)$_2$].

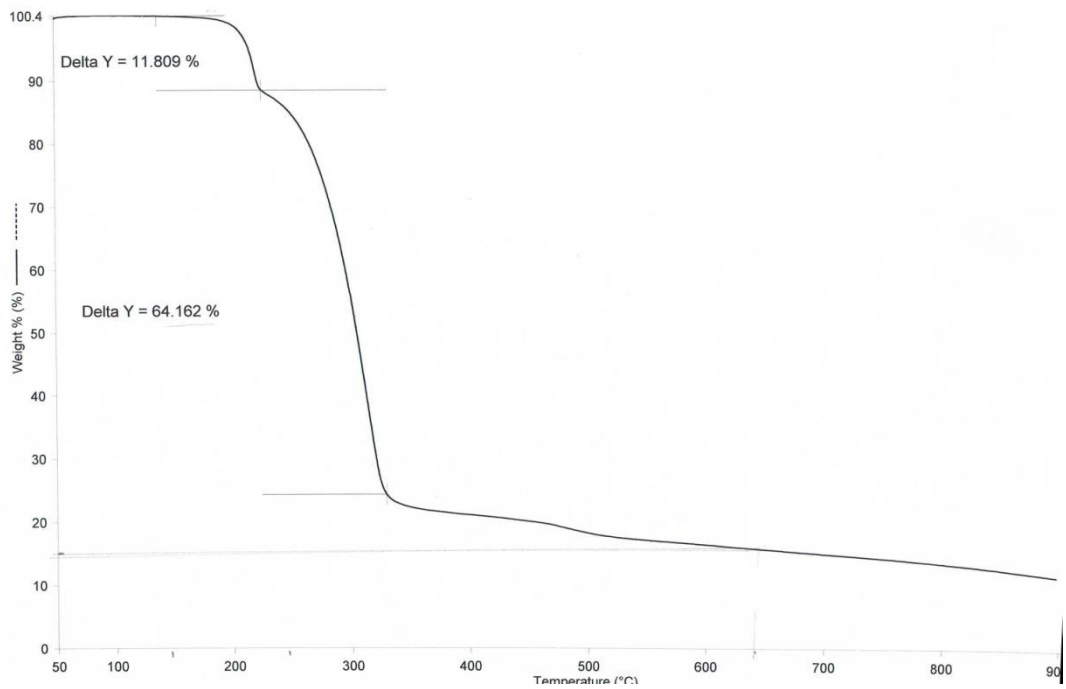

Figure 4.58 TGA for [CuL4(H_2O)]

Based on the above analytical results, the proposed structure for [CuL4(H_2O)] is shown in **Figure 4.59.**

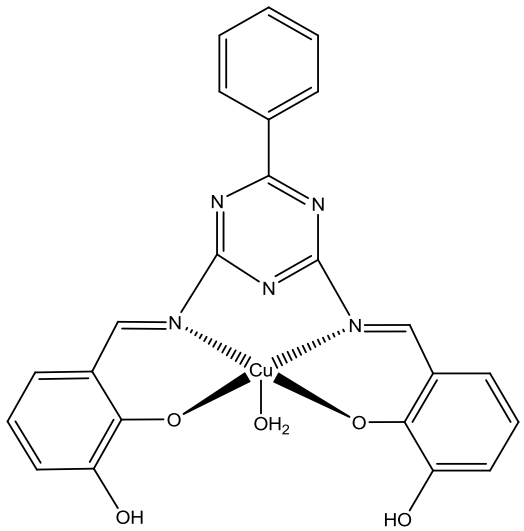

Figure 4.59 Proposed structural formula of [CuL4(H_2O)]

4.5.4 Zinc(II) complex of H_2L4

The zinc(II) complex was obtained as a pale yellow powder in good yield (77%) in the reaction between H_2L4 and zinc(II) acetate dihydrate in presence of triethylamine. The yield is similar to Cu(II) complex (73%) , indicating similar solubility in ethanol.

The results from the **CHN** elemental analyses are in excellent agreement with the expected chemical formula $ZnC_{23}H_{15}O_4N_5$ or $[ZnL4].2H_2O$.

The **FTIR** spectrum of $[ZnL4].2H_2O$ (**Figure 4.60**) shows the presence of all the expected functional groups. The wavenumbers of C=N (1621 cm^{-1}) and C-O (1257 cm^{-1}) groups are almost the same as for $[CuL4(H_2O)]$ (1624 cm^{-1} and 1258 cm^{-1} respectively.

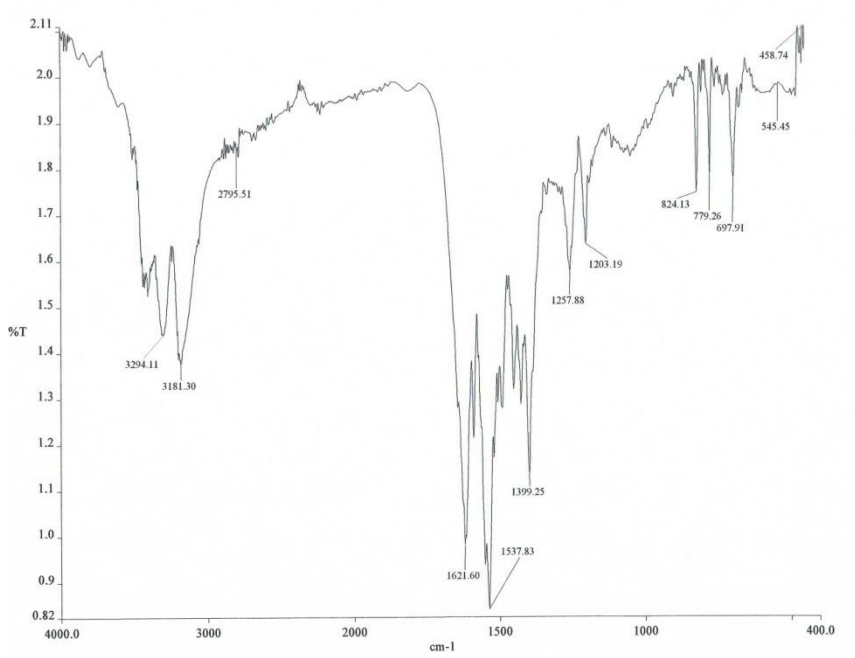

Figure 4.60 FTIR spectrum of $[ZnL4].2H_2O$

The **UV-vis** spectrum of $[ZnL4].2H_2O$ (**Figure 4.61**) shows that the MLCT and π-π^* peaks 414 nm (ε_{max} = 0.28 x 10^4 $M^{-1}cm^{-1}$), and 291 nm (ε_{max} = 1.7 x 10^4 $M^{-1}cm^{-1}$) are at almost the same energy as the corresponding peaks for $[CuL4(H_2O)]$ (420 nm, 260 nm; **Figure 4.57**).

Thus, both metal ions have insignificant effect on the electronic transitions of the organic moiety. The MLCT peak is normally observed from 348 nm to 323 nm for Zn(II) complexes, involving electronic transitions from the full *d* orbitals of the metal ion ($3d^{10}$) to antibonding orbitals of the ligand [75].

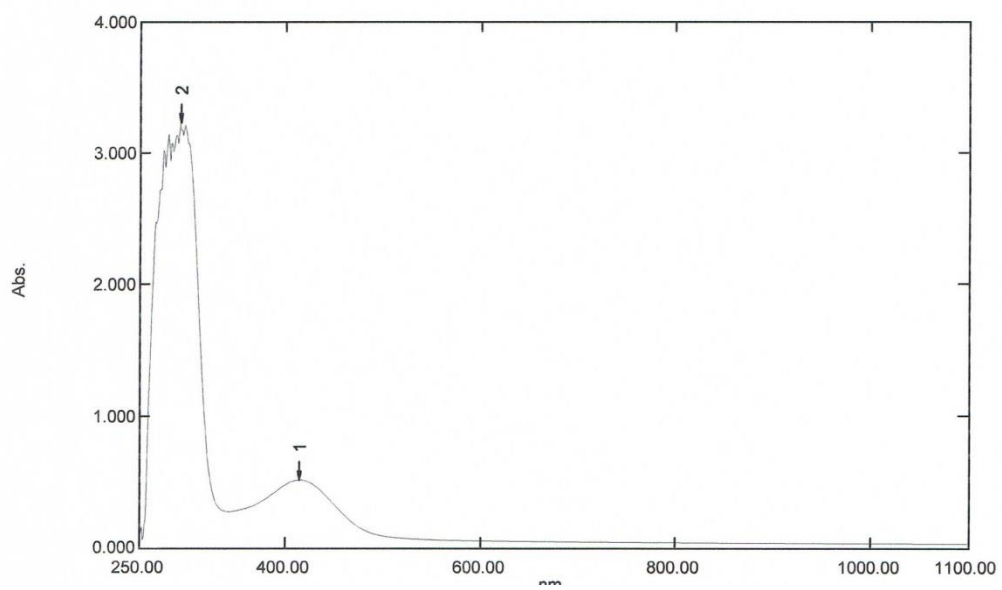

Figure 4.61 UV-vis spectrum of [ZnL4].2H_2O

The **TGA** thermogram **(Figure 4.62**), measured from 50^oC up to 900^oC, shows that the complex was stable up to 210^oC. Thus, it is as themally stable as [CuL4(H_2O)] (205^oC).

The first weight loss of 4.3% at 190^oC corresponds to the loss of coordinated H_2O molecules (expected, 6.8%). The next step represents a total weight loss of 82% and is assigned to the decomposition of the ligand (expected, 81.1%). The amount of residue at 850^oC is 13.7%. Assuming that the residue is ZnO [73], the expected value is 15.3%, which is within the acceptable experimental error.

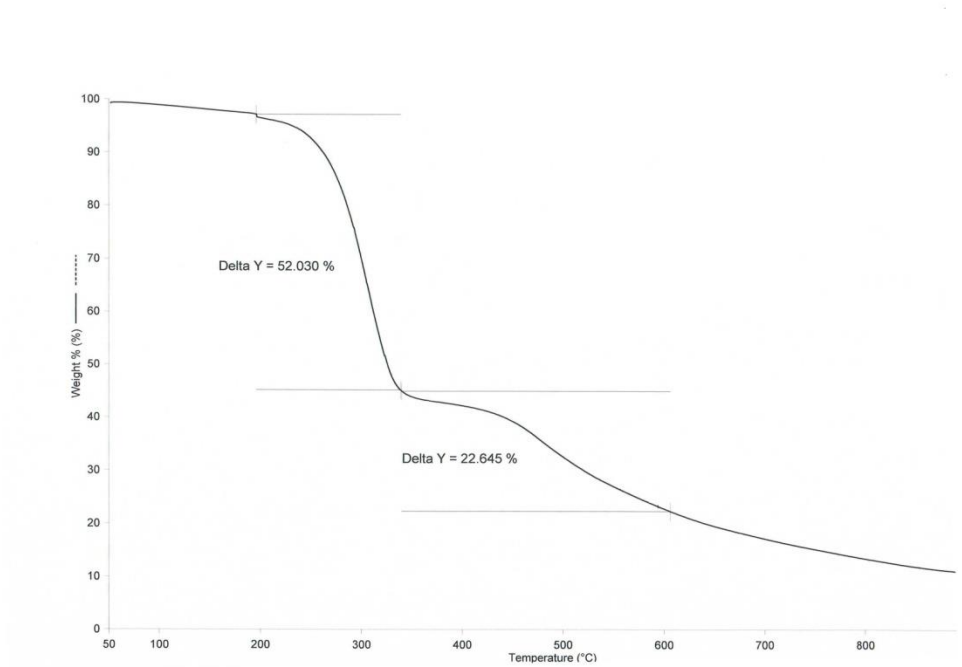

Figure 4.62 TGA for [ZnL4].2H_2O

Based on the above analytical results, and on the knowledge that Zn(II) prefers tetrahedral geometry, the proposed structure for [ZnL4].2H_2O is shown in **Figure 4.63.**

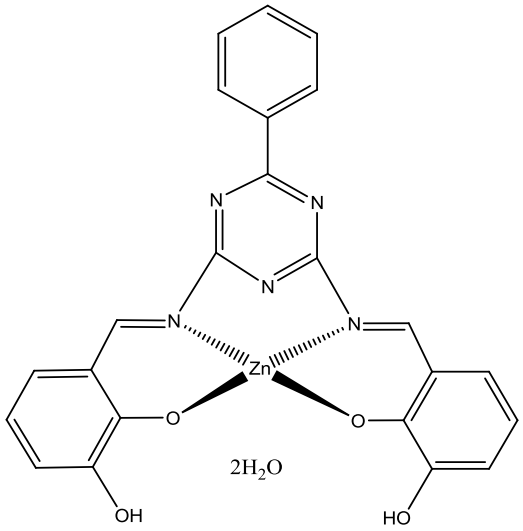

Figure 4.63 Proposed structural formula of [ZnL4].2H_2O (the solvate H_2O is not shown)

4.6 H_2L5 and its Ni(II), Cu(II) and Zn(II) complexes

4.6.1 H_2L5

H_2L5 was obtained as an orange powder in good yield (78%) from the reaction shown in **Scheme 4.1** (X =4-OH). The yield is similar to that of H_2L4 (76%), indicating similar solubility in ethanol. The results from the CHN elemental analysis are in excellent agreement with the chemical formula, $C_{23}H_{17}O_4N_5$.

The **FTIR** spectrum (**Figure 4.64** shows the presence of all of the expected functional groups at almost the same wavenumbers as discussed for H_2L4. Thus, replacing 4-OH has no significant effect on the bond strengths of C=N and C-O functional groups of the Schiff base.

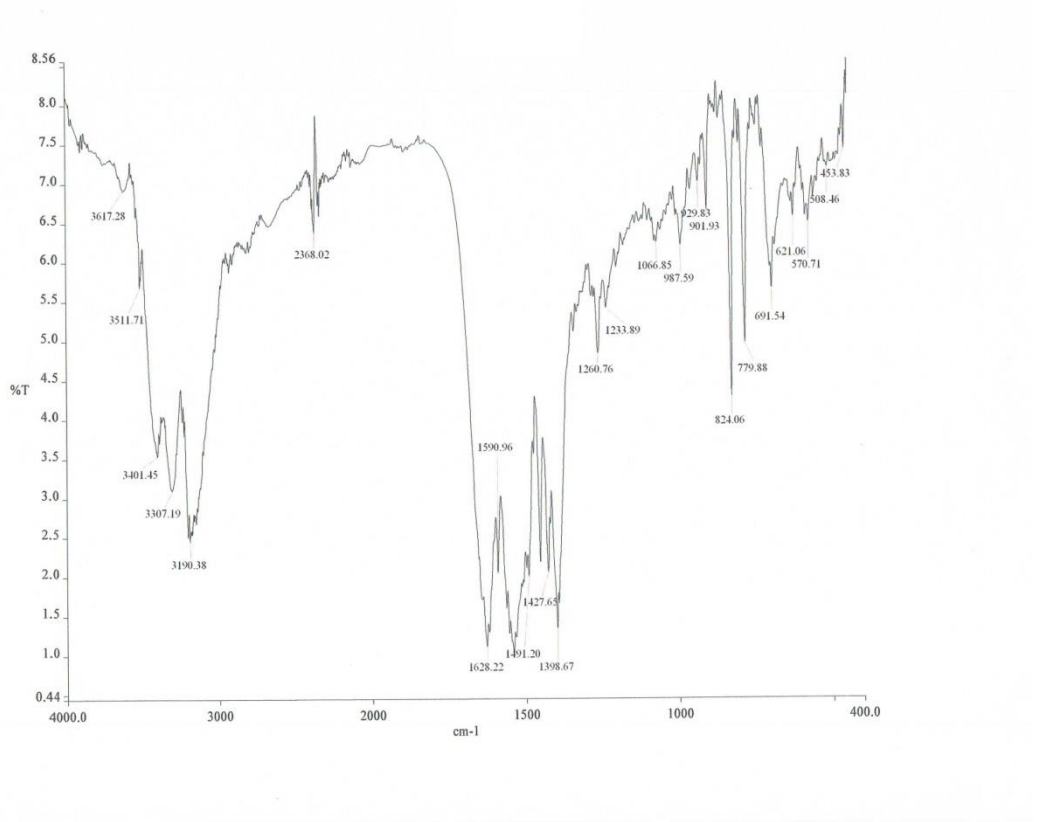

Figure 4.64 FTIR spectrum of H_2L5

The **^{1}H-NMR** spectrum (**Figure 4.65) is** consistent with the expected structural formula of H_2L5: a singlet at 10.13ppm is due to phenolic hydrogen; a singlet at 8.19 ppm is due to imino hydrogen; and a multiplet in the range 6.70 - 7.43 ppm is due to the aromatic hydrogens. The integration ratio for these hydrogens is 2:1:5.5 respectively (expected ratio =2:1:5.5) The results support the molecular symmetry for the Schiff base, and indicate insignificant electronic effects when 3-OH (H_2L4) is replaced by 4-OH (H_2L5).

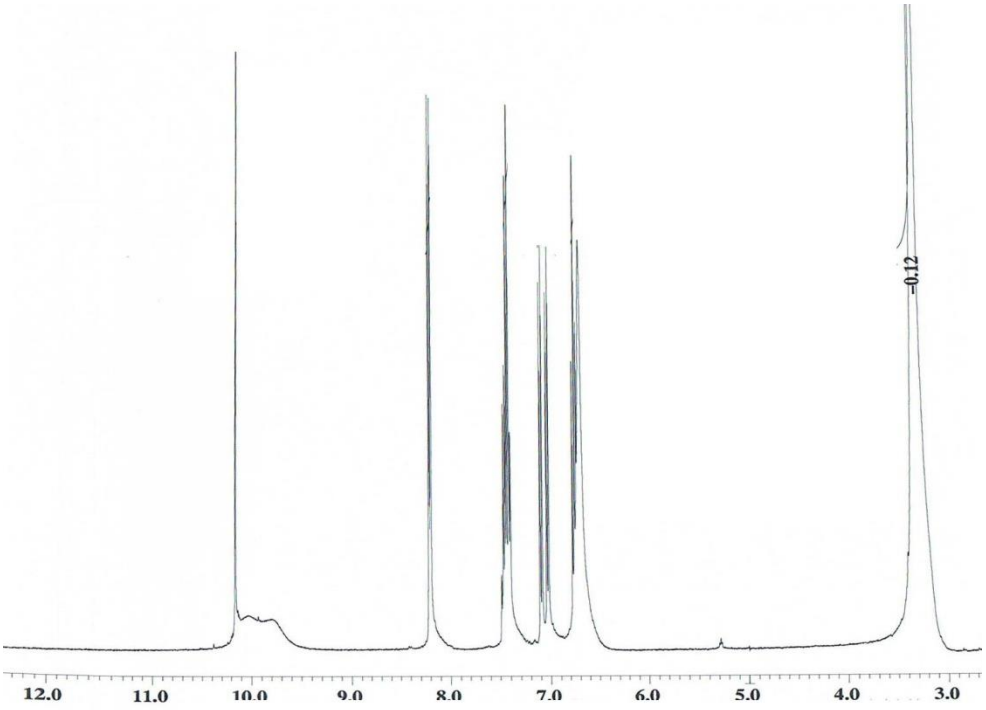

Figure 4.65 ^{1}H-NMR spectrum of H_2L5

The **^{13}C-NMR** spectrum (**Figure 4.66**) shows 12 peaks, assigned as follows (in ppm): 120.4, 124.5, 137.6 and 140 phenol, 128.1, 128.7, 131.0, 131.6 phenyl ring, 170.6 triazine ring, and 160.3 C=N. Other peaks are overlapping.

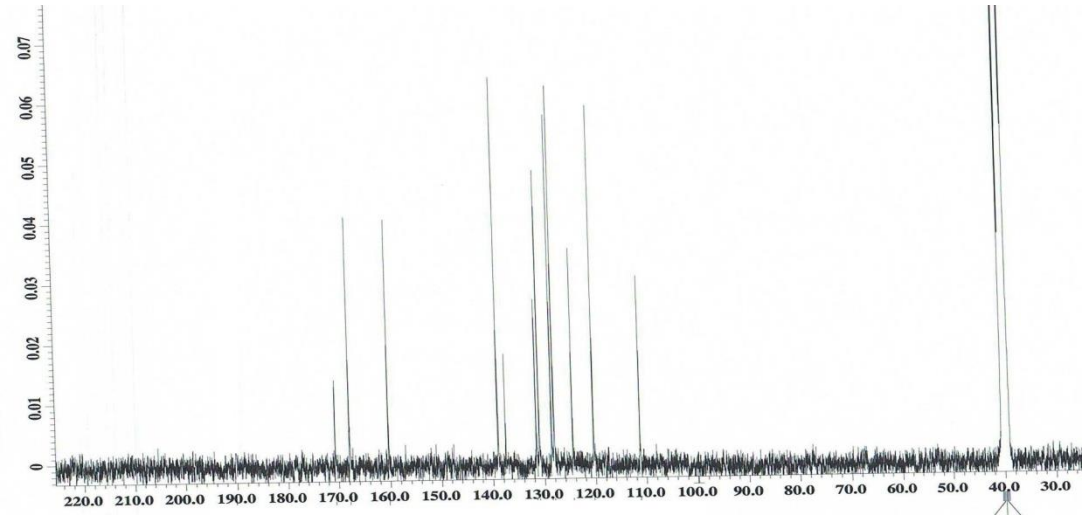

Figure 4.66 ^{13}C-NMR spectrum of H_2L5

The **UV-vis** spectrum of a solution of H_2L5 in DMSO (**Figure 4.67**) shows that the peak assigned to the π-π^* transition (282 nm; ε, 1.4x10^4 M^{-1}cm^{-1}), while the peak for the n-π^* transition (310 nm; ε, 1.7x10^4 M^{-1}cm^{-1}) has shifted to higher energy compare to those of H_2L4 (286 nm, 344 nm respectively) [65].

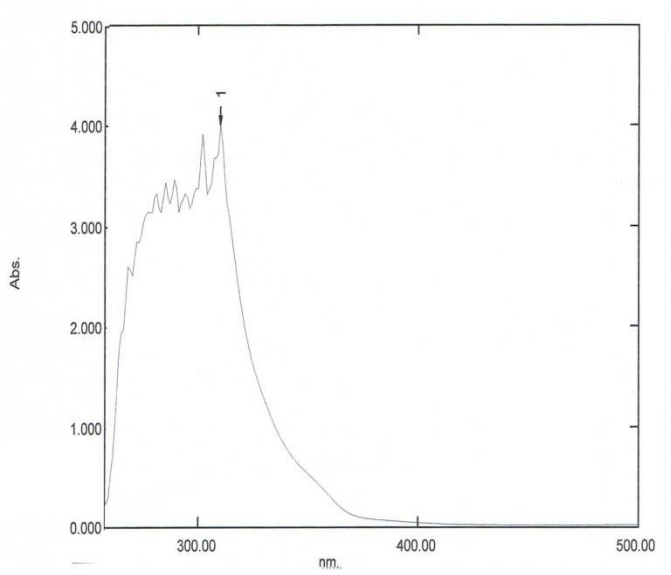

Figure 4.67 UV-vis spectrum of H_2L5 in DMSO

4.6.2 Nickel(II) complex of H_2L5

The nickel(II) complex was obtained as a light-green powder in good yield (76%) in the reaction between H_2L5 and nickel(II) acetate tetrahydrate in presence of triethylamine. The yield is similar to that of $[NiL4(H_2O)_2]$ (72%), indicating similar solubility in ethanol.

The results from the **CHN** elemental analyses are in excellent agreement with the chemical formula, $[Ni(C_{23}H_{15}O_4N_5)(H_2O)_2]$ or $[NiL5(H_2O)_2]$.

The **FTIR** spectrum (**Figure 4.68**) differs from that of H_2L5 (**Figure 4.64**). It is further noted that the -OH peak, observed for H_2L5 at 3401 cm^{-1}, is now observed at 3301 cm^{-1}, and is assigned to coordinated H_2O molecules in agreement with the results from the elemental analyses [74]. The peaks for C=N at 1628 cm^{-1} and C-O at 1260 cm^{-1} observed for H_2L5 are observed at 1622 cm^{-1} and 1269 cm^{-1} respectively in $[NiL5(H_2O)_2]$. The Ni-O peak is observed at 568 cm^{-1}. These suggest that the phenolic oxygens and imino nitrogens are coordinated to Ni(II). Also, it is noted that the strengths of C=N and C-O bonds are similar for $[NiL5(H_2O)_2]$ (1622 cm^{-1}; 1269cm^{-1} respectively) compared to those of $[NiL4(H_2O)_2]$ (1622 cm^{-1}; 1255 cm^{-1} respectively).

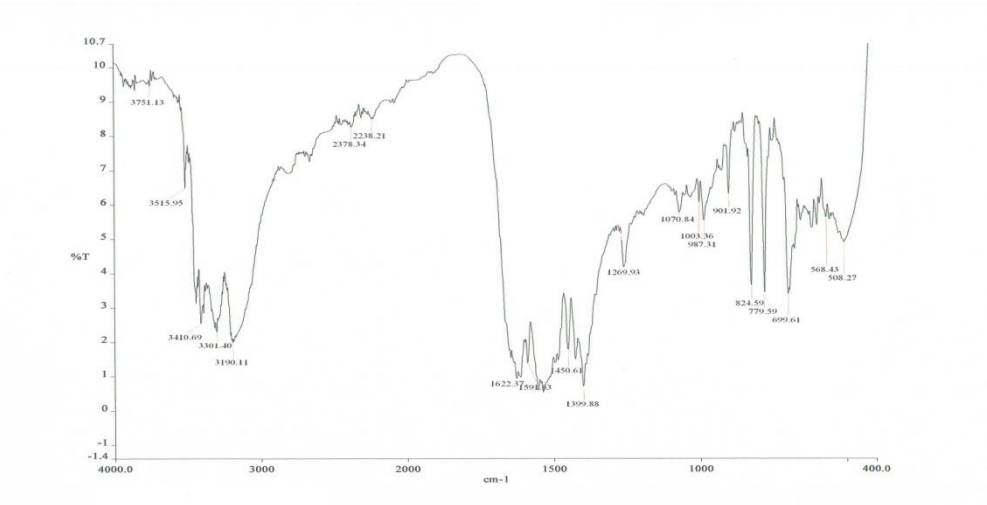

Figure 4.68 FTIR spectrum of $[NiL5(H_2O)_2]$

The **UV-vis** spectrum of [NiL5$(H_2O)_2$] (**Figure 4.69**) shows *d-d* bands at 902nm (ε_{max} = 405 $M^{-1}cm^{-1}$), and 737 nm (ε_{max} = 189 $M^{-1}cm^{-1}$). These are consistent with an octahedral configuration at Ni(II), and these bands are similarly assigned as for [NiL4$(H_2O)_2$]. The peak at 296 nm ($\varepsilon = 2.1x\ 10^4\ M^{-1}cm^{-1}$) is assigned to π - π^* transition of the aromatic ring.

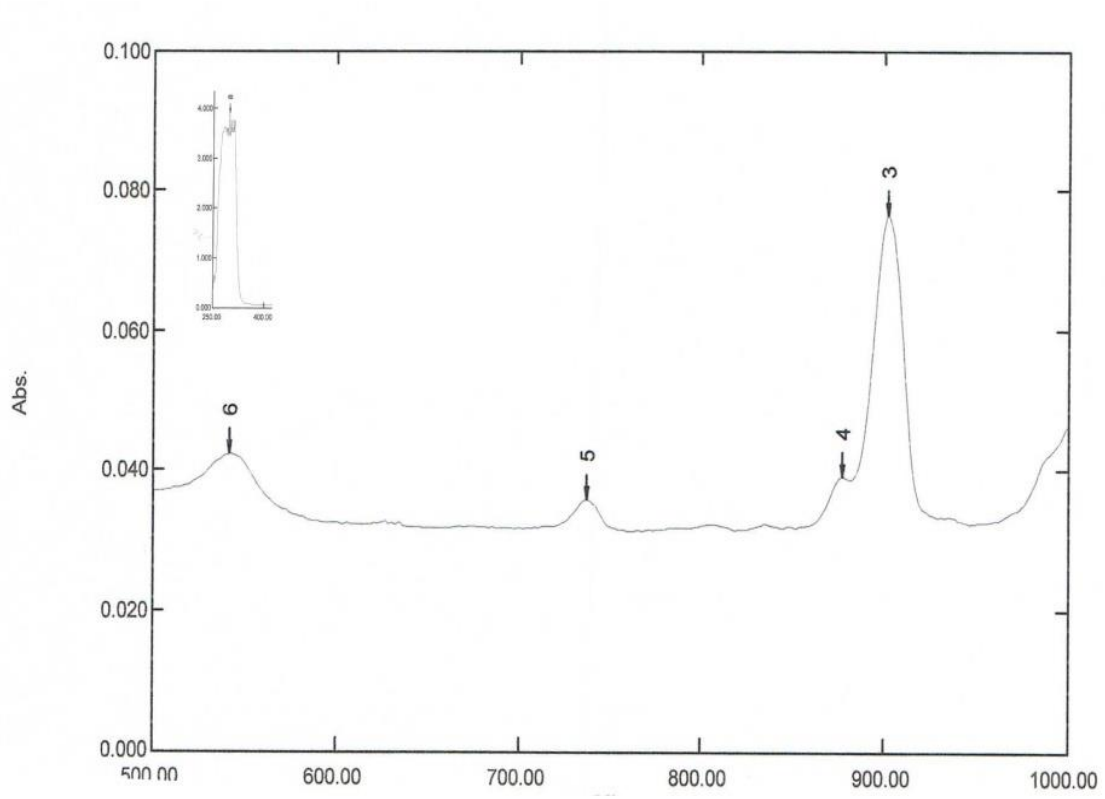

Figure 4.69 UV-vis spectrum of [NiL5$(H_2O)_2$] in DMSO

The **TGA** thermogram **(Figure 4.70)**, measured from 50^oC up to 900^oC, shows that the complex was stable up to 205^oC. Thus, it is slightly similar thermally stable for [NiL4$(H_2O)_2$] (200^oC)**.**

The first weight loss of 2.9% at 142^oC corresponds to the loss of coordinated H_2O molecules (expected, 6.9%). The next step represents a total weight loss of 81.6% and is assigned to the decomposition of the ligand (expected, 82.1%). The amount of residue at

temperatures above 720°C is 15.6%. Assuming that the residue is NiO [73], the expected value is 14.5%, which is within the acceptable experimental error.

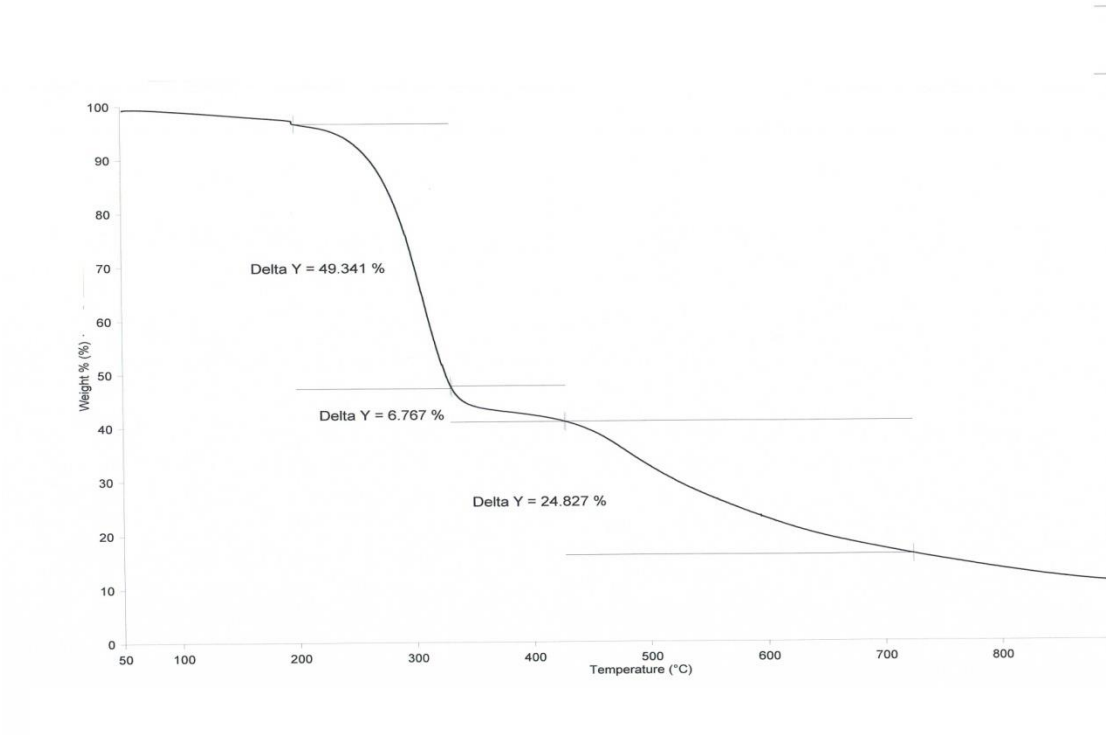

Figure 4.70 TGA for [NiL5(H_2O)$_2$]

Based on the above analytical results, the proposed structure for [NiL5(H_2O)$_2$] is similar to that of [NiL4(H_2O)$_2$] (**Figure 4.55**).

4.6.3 Copper(II) complex of H_2L5

The copper(II) complex was obtained as a light green powder in good yield (71%) in the reaction between H_2L5 and copper(II) acetate monohydrate in presence of triethylamine. The yield is similar to [CuL4(H_2O)] (73%), indicating similar solubility in ethanol.

The results from the **CHN** elemental analyses are in excellent agreement with the expected chemical formula $CuC_{23}H_{15}O_4N_5$ or [CuL5(H_2O)].

The **FTIR** spectrum (**Figure 4.71**) shows the expected functional groups as previously discussed for [CuL4(H_2O)] (**Figure 4.56**). The C=N and C-O peaks for [CuL5(H_2O)] are at 1626 cm^{-1} and 1264 cm^{-1} respectively. These are almost similar to those of [CuL4(H_2O)] (1624 cm^{-1} and 1258 cm^{-1}), suggesting similar bond strength.

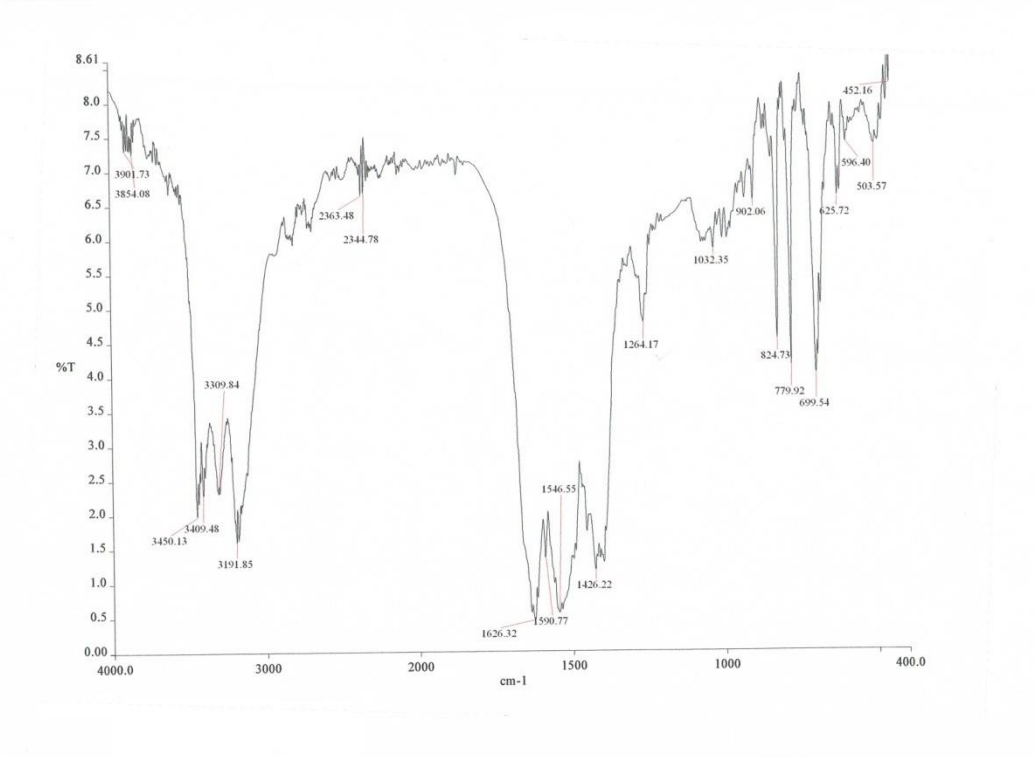

Figure 4.71 FTIR spectrum of [CuL5(H_2O)]

The **UV-vis** spectrum (**Figure 4.72**) shows a broad *d-d* peak at 685 nm (ε_{max} = 200 M^{-1} cm^{-1}). Thus, [CuL5(H_2O)] is a mononuclear square pyramidal complex. The band π-π^* is at 279 nm (ε_{max} = 2.1x10^4 $M^{-1}cm^{-1}$) which is almost the same as for the corresponding and [CuL4(H_2O)], may be similarly explained.

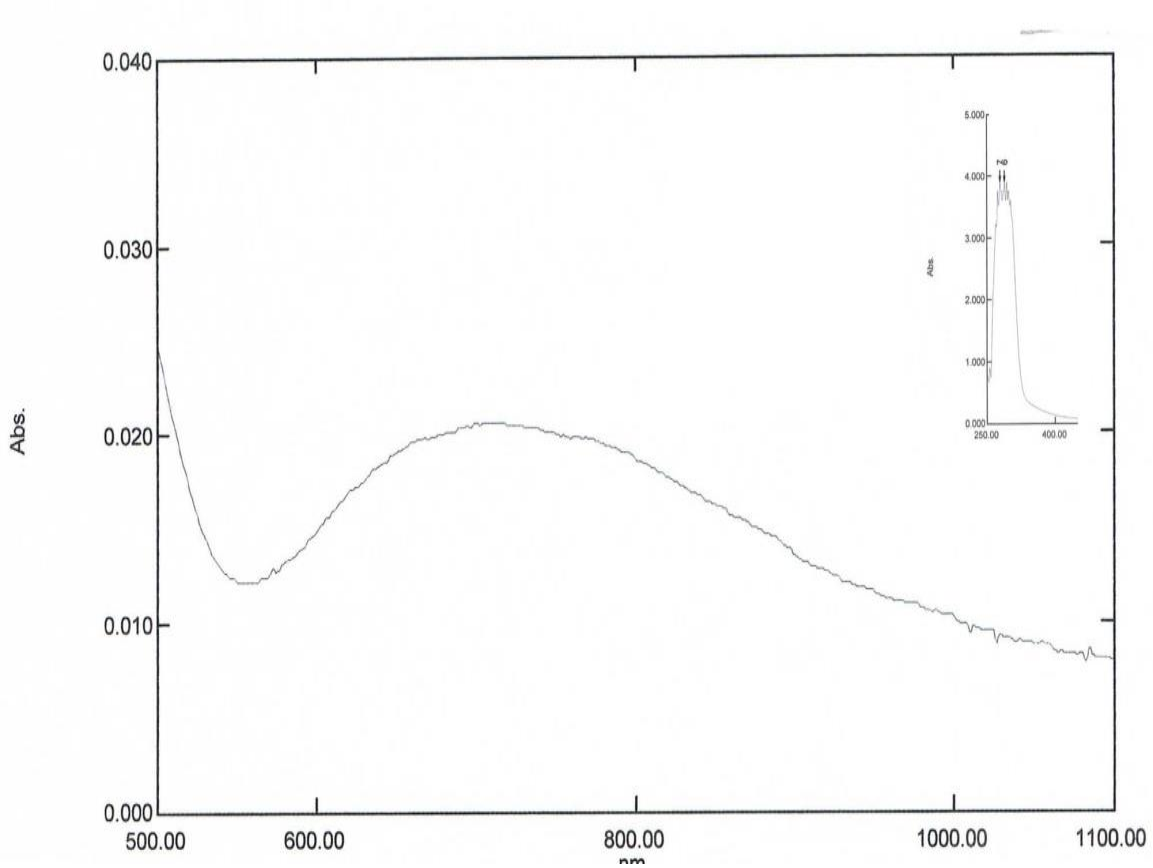

Figure 4.72 UV-vis spectrum of [CuL5(H_2O)]

The **TGA** thermogram **(Figure 4.73)**, measured from 50^oC up to 900^oC, shows that the complex was stable up to 260^oC. Thus, it is more thermally stable than [CuL4(H_2O)] (205^oC). Thus, changing the position of OH from *meta* position to *para* position of the phenolic ring has increased the thermal stability of the complex. This may be due to the formation of intermolecular H-bonding in [CuL5(H_2O)], while there was only intramolecular H-bonding in [CuL4(H_2O)].

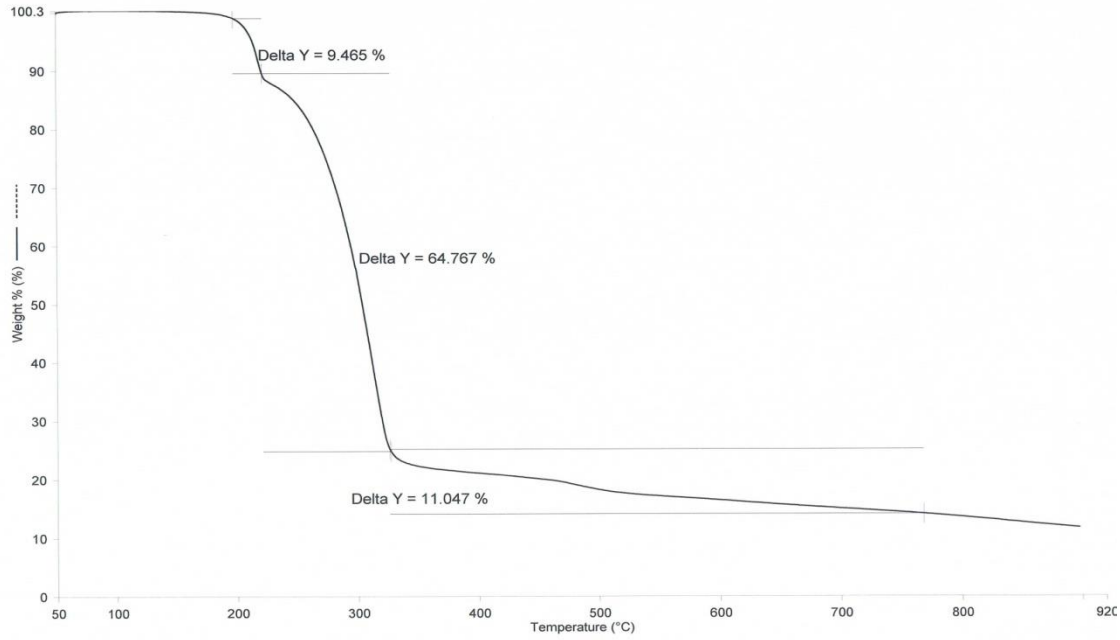

Figure 4.73 TGA for[CuL5].H_2O

The first weight loss of 4.5% at 148^{o}C corresponds to the loss of coordinated H_2O molecules (expected, 3.5%). The next step represents a total weight loss of 80.4% and is assigned to the decomposition of the ligand (expected, 84.6%). The amount of residue at 770 ^{o}C is 14.9%. Assuming that the residue is CuO, the expected value is 15.7%, which is within the acceptable experimental error.

Based on the above analytical results, the proposed structure for [CuL5(H_2O)] is similar to the previously discussed copper(II) complexes, [CuL4(H_2O)] (**Figure 4.59**).

4.6.4 Zinc(II) complex of H_2L5

The zinc(II) complex was obtained as a light yellow powder in good yield (79%) in the reaction between H_2L5 and zinc(II) acetate dihydrate in presence of triethylamine. The yield is similar to that of $[ZnL4].2H_2O$ (77%), suggesting similar solubility in ethanol.

The results from the **CHN** elemental analyses are in excellent agreement with the expected chemical formula $ZnC_{23}H_{15}O_4N_5$ or $[ZnL5].2H_2O$.

The **FTIR** spectrum of $[ZnL5].2H_2O$ (**Figure 4.74**) shows the presence of all the expected functional groups. The wave numbers of C=N (1618 cm^{-1}) and C-O (1258 cm^{-1}) groups are almost the same as for $[ZnL4].2H_2O$ (1621cm^{-1} and 1257 cm^{-1} respectively. Thus, the C=N and C-O bond strengths are similar in both complexes.

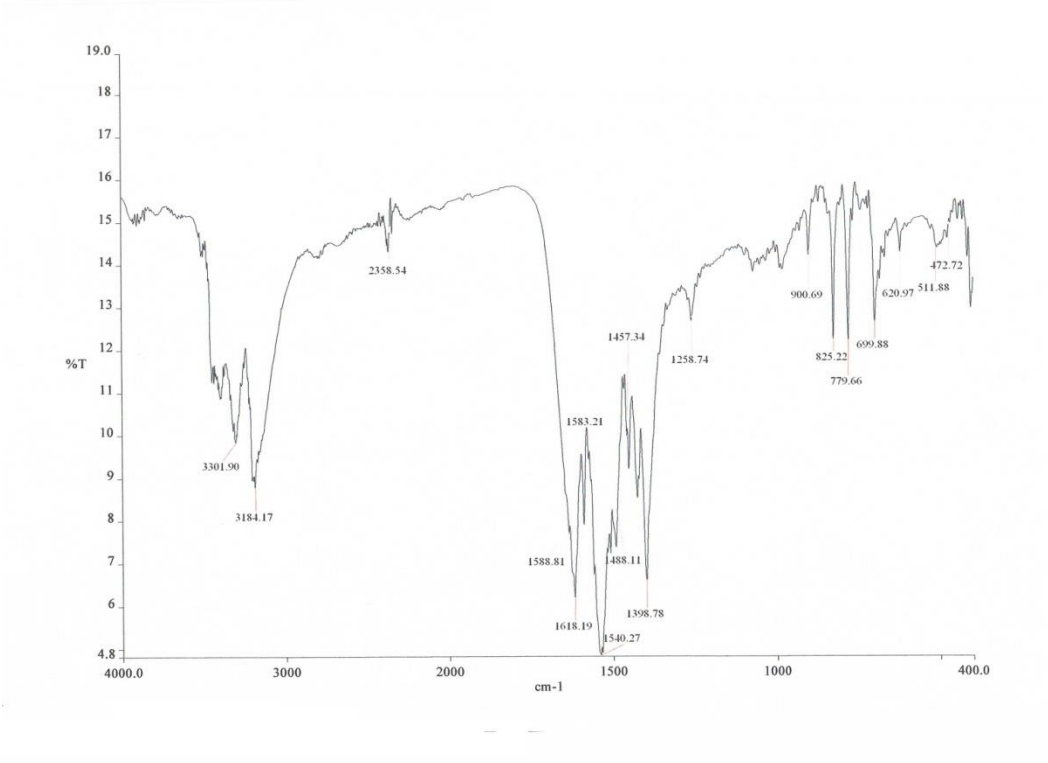

Figure 4.74 FTIR spectrum of $[ZnL5].2H_2O$

The **UV-vis** spectrum of [ZnL5].2H_2O (**Figure 4.75**) shows that the band π-π^* is at 296 nm (ε_{max} = 1.9x10^4 $M^{-1}cm^{-1}$) which is almost the same as for the corresponding peak for [ZnL4].2H_2O (291 nm(ε_{max} = 1.7x10^4 $M^{-1}cm^{-1}$; **Figure 4.61**). Thus, substituting 3-OH for 4-OH at the 4-position of the phenolic ring has no significant effect on the electronic transitions of the organic moiety.

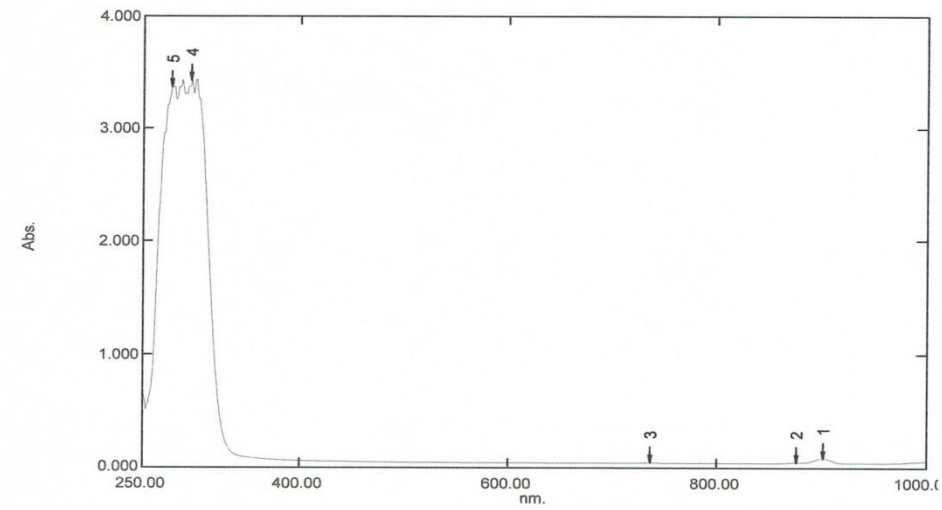

Figure 4.75 UV-vis spectrum of [ZnL5].2H_2O

The **TGA** thermogram **(Figure 4.76**), measured from 50^oC up to 900^oC, shows that the complex was stable up to 206^oC. Thus, it is as thermally stable as [ZnL4].2H_2O (210^oC). Thus, substituting 3-OH for 4-OH at the 4-position of the phenolic ring has no significant effect on the structure of the complex.

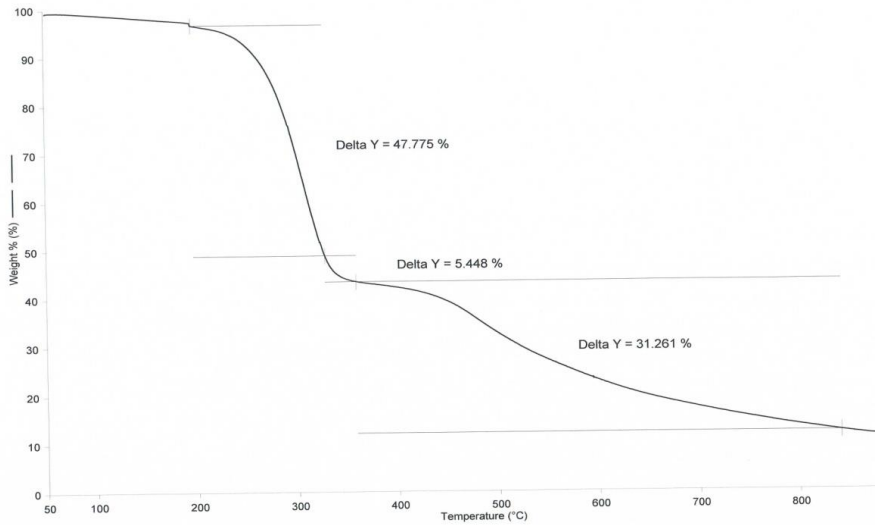

Figure 4.76 TGA for [ZnL5].2H_2O

The first weight loss of 4.1% at 185^oC corresponds to the loss of coordinated H_2O molecules (expected, 6.8%). The next step represents a total weight loss of 81.8% and is assigned to the decomposition of the ligand (expected, 81.1%). The amount of residue at 840^oC is 13.8%. Assuming that the residue is ZnO [73], the expected value is 15.3%, which is within the acceptable experimental error.

Based on the above analytical results, the proposed structure for [ZnL5].2H_2O is similar to the previously discussed zinc(II) complexes, [ZnL4].2H_2O (**Figure 4.63**).

4.7 H_2L6 and its Ni(II), Cu(II) and Zn(II) complexes

4.7.1 H_2L6

H_2L6 was obtained as a pale yellow powder in good yield (81%) from the reaction shown in **Scheme 4.1** (X = 3,5-$(C(CH_3)_3)_2$). The results from the CHN elemental analysis are in excellent agreement with the chemical formula, $C_{39}H_{49}O_2N_5$.

The **FTIR** spectrum (**Figure 4.77)** shows the characteristics strong peak due to C=N stretching at 1612 cm^{-1}, indicating the formation of the Schiff base. Another strong peak at 1273 cm^{-1} is assigned to C-O phenolic stretching, while a sharp weak peak at 3329 cm^{-1} is characteristic of free -OH group [70]. Other peaks bands in the region 1000 - 1500 cm^{-1} arise from benzene ring skeletal vibrations.

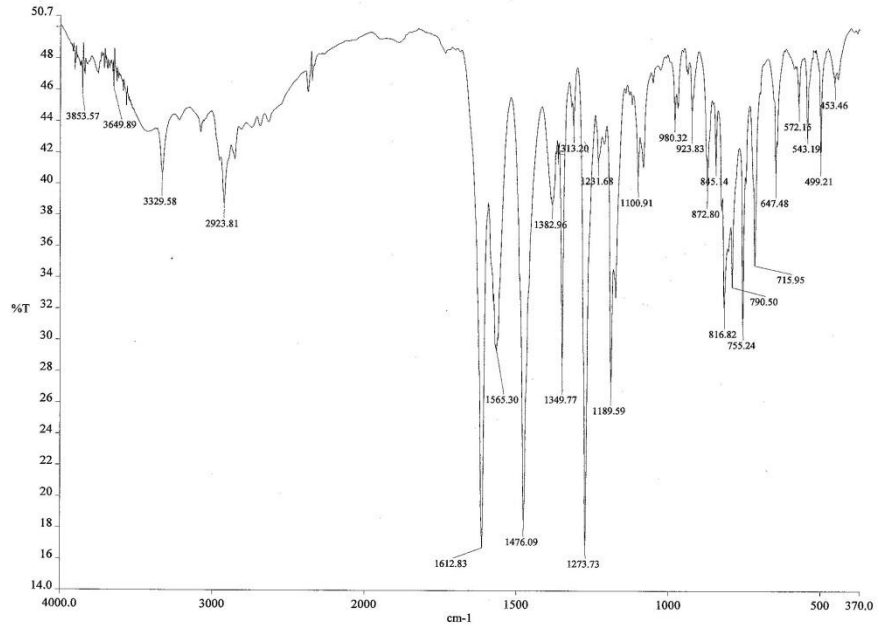

Figure 4.77FTIR spectrum of H_2L6

The **^{1}H-NMR** spectrum (**Figure 4.78) is** consistent with the expected structural formula of H_2L6: a singlet at 9.96ppm is due to phenolic hydrogen; a singlet at 8.24 ppm is due to imino hydrogen; and a multiplet in the range 6.70 - 7.61 ppm is due to the aromatic hydrogens. Furthermore a singlet at 1.33 ppm is due to tertiary butyl protons. The integration ratio for these hydrogens is 1:1:5.5 respectively (expected ratio =1:1:5.5), and supports the molecular symmetry for the Schiff base [68].

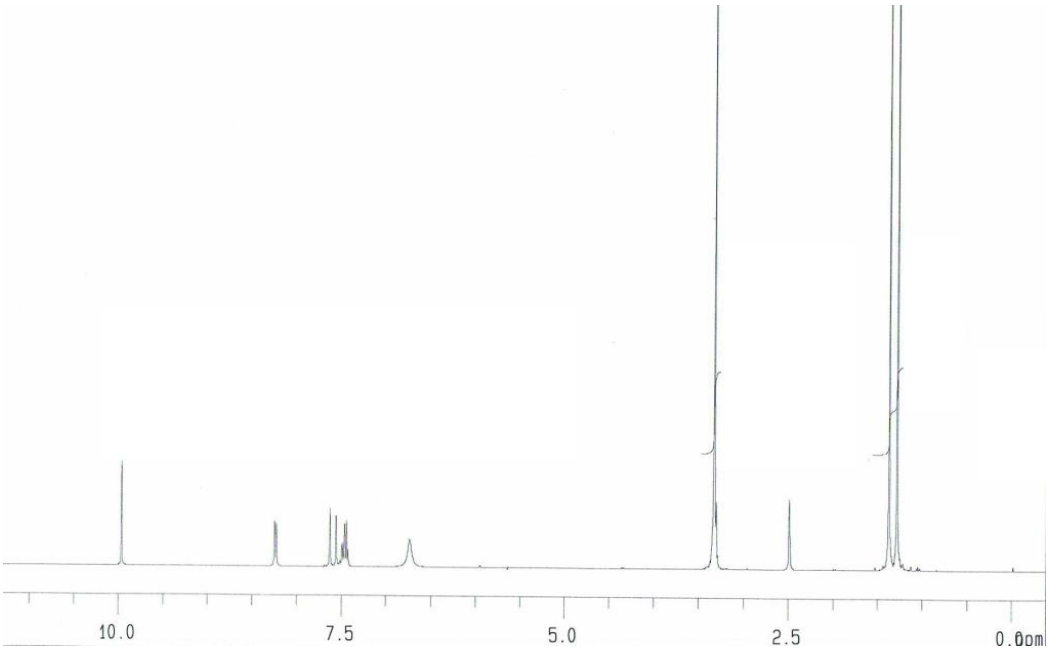

Figure 4.78 ^{1}H-NMR spectrum of H_2L6

The **^{13}C-NMR** spectrum (**Figure 4.79**) shows 15 peaks, assigned as follows: 29 ppm (tertiary carbon atoms in the tert-butyl groups), 31.8 ppm for the six methyl groups, 159.4 ppm C-OH, 167.91 ppm C=N, The aromatic carbons lie between 120.6 – 141.9 ppm. However, the expected number of peaks, after taking account of the symmetry of the structure, is 15.

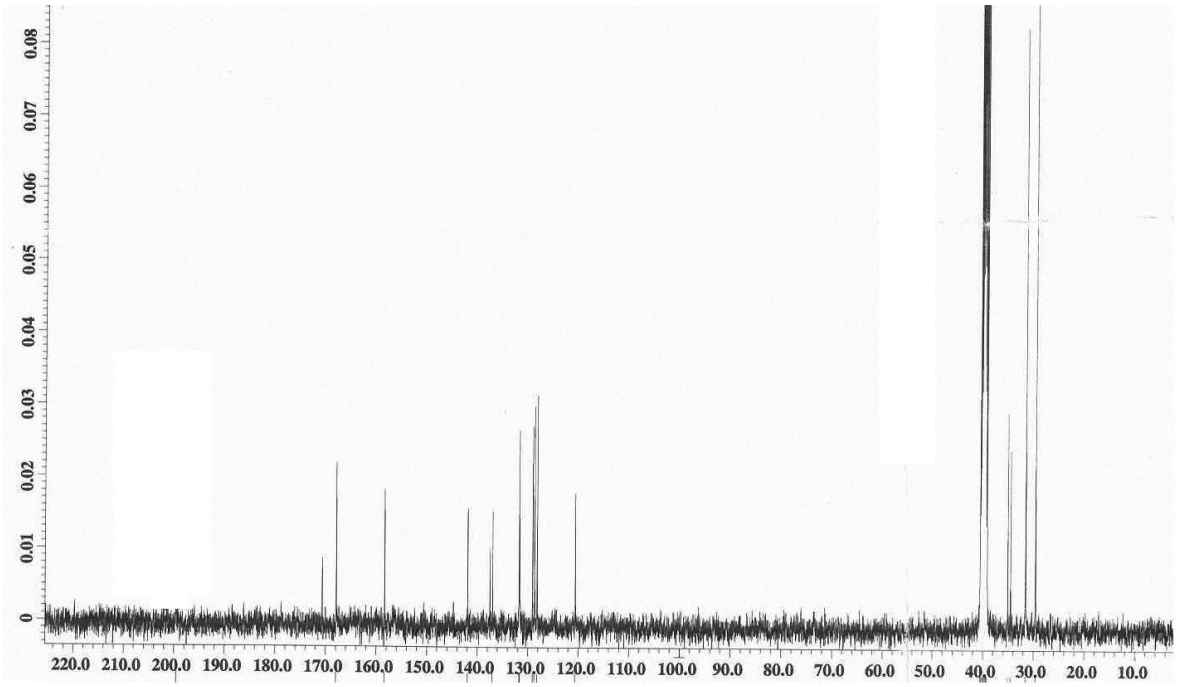

Figure 4.79 ^{13}C-NMR spectrum of H_2L6

The **UV-vis** spectrum of a solution of H_2L6 in DMSO (**Figure 4.80)** shows two moderately intense absorption bands at 288 nm ($\varepsilon = 2.1x10^4$ $M^{-1}cm^{-1}$) and 351 nm ($\varepsilon = 2.2 \times 10^4$ $M^{-1}cm^{-1}$). The bands are assigned to π-π^* transition of the aromatic ring and *n*-π^* transition of the azomethine chromophores, respectively. These values are in agreement with other Schiff bases reported in the literatures [71].

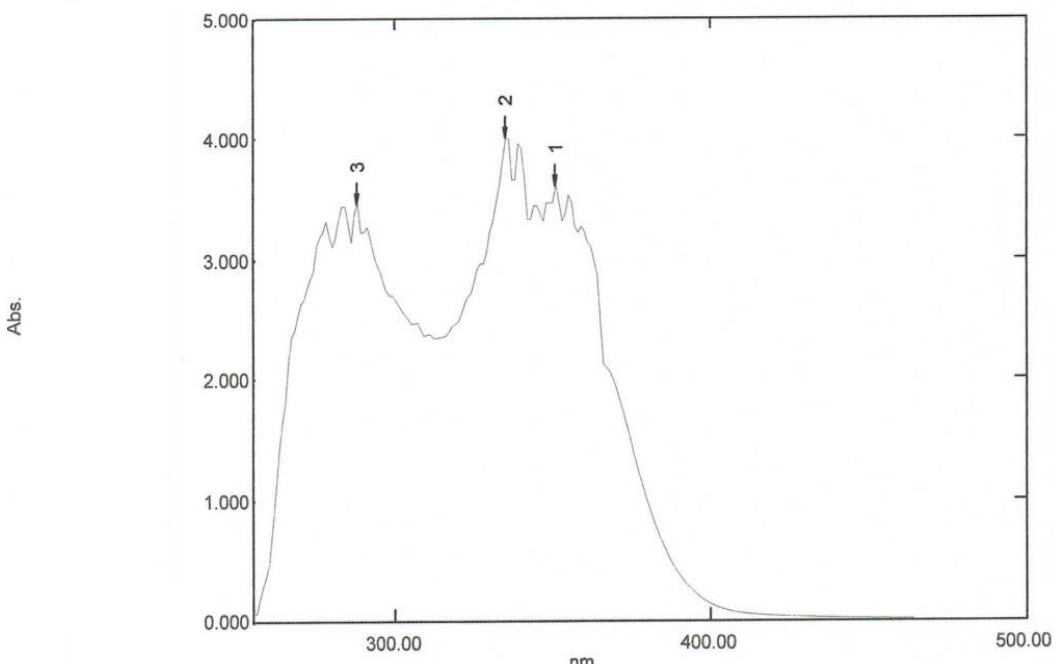

Figure 4.80 UV-vis spectrum of H_2L6 in DMSO

4.7.2 Nickel(II) complex of H_2L6

The nickel(II) complex (NiL6) was obtained as a light green powder in good yield (75%) in the reaction between H_2L6 and nickel(II) acetate tetrahydrate in presence of triethylamine.

The results from the **CHN** elemental analyses are in excellent agreement with the chemical formula, $[Ni(C_{39}H_{47}O_2N_5)(H_2O)_2]$ or $[NiL6(H_2O)_2]$.

The **FTIR** spectrum of NiL6 (**Figure 4.81**) is compared with that of H_2L6 (**Figure 4.77**). It is further noted that the -OH peak, observed for H_2L6 at 3329cm^{-1}, is now observed at 3401 cm^{-1}, and is assigned to coordinated H_2O molecules in agreement with the results from the elemental analyses . The peaks for C=N at 1612 cm^{-1} and C-O at 1273 cm^{-1} observed for H_2L6 have shifted to lower energy at 1606cm^{-1} and 1239cm^{-1} respectively in NiL6. These suggest that

the phenolic oxygens and imino nitrogens are coordinated to Ni(II). Additionally, a new peak observed at 550 cm^{-1} may be assigned to Ni-O bond [74].

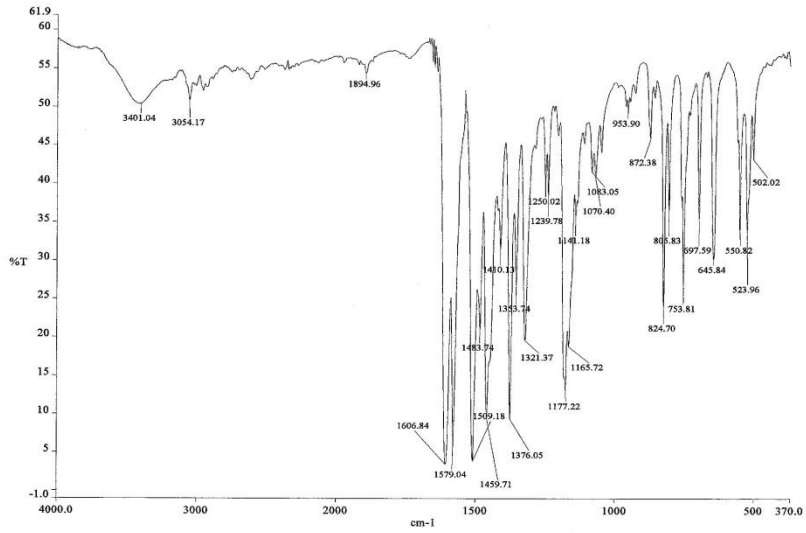

Figure 4.81 FTIR spectrum of $[NiL6(H_2O)_2]$

The **UV-vis** spectrum (**Figure 4.82;** shown as insert) shows weak *d-d* bands 902 nm (ε_{max} = 550 $M^{-1}cm^{-1}$), and 736 nm (ε_{max} = 257 $M^{-1}cm^{-1}$). These are consistent with an octahedral configuration at Ni(II).

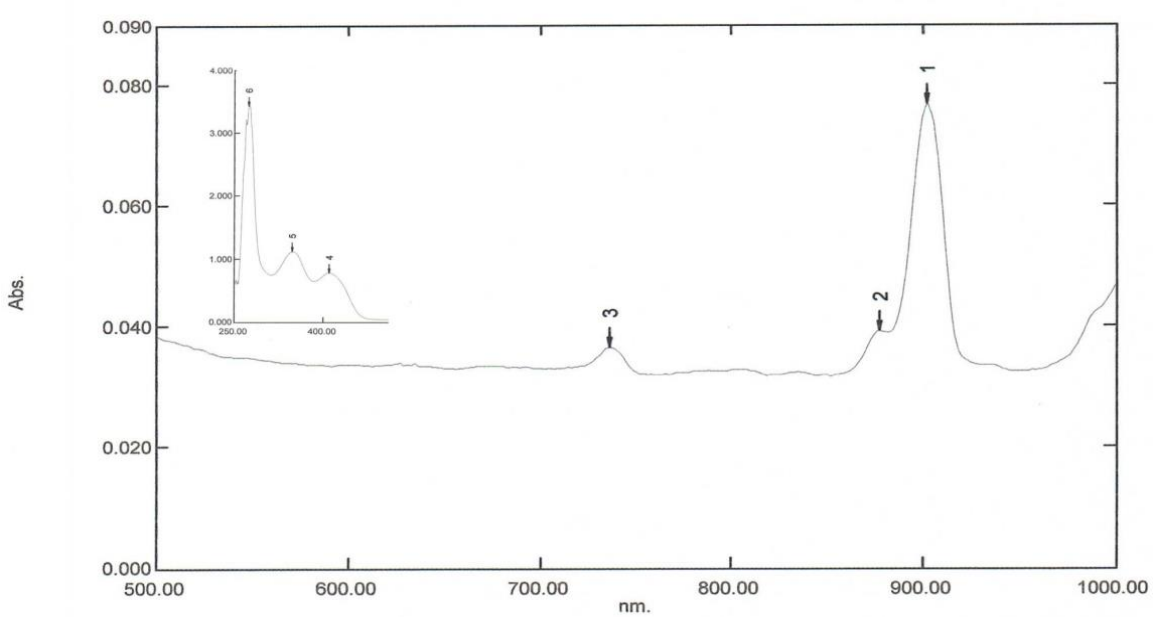

Figure 4.82 UV-vis spectrum of [NiL6(H_2O)$_2$] in DMSO

The peak at 410 nm (ε = 0.5 x 10^4 $M^{-1}cm^{-1}$) is assigned to metal-ligand charge transfer (MLCT). The spectrum is also compared with that of H_2L6 (**Figure 4.80**).It is noted that the π-π* band observed for H_2L6 (288 nm) remains shifted in the complex (274 nm) (ε = 2.4x 10^4 M^{-1} cm^{-1}). However, the *n*-π* band may be hidden under the strong MLCT band at 348 nm (ε = 0.7 x 10^4 $M^{-1}cm^{-1}$). Thus, this band is significantly red-shifted from about 300 nm to about 400 nm as a result of complexation to the Ni(II). These results are in agreement with literature result indicating the formation of the complex [82].

The **TGA** thermogram **(Figure 4.83**), measured from 50^{o}C up to 900^{o}C, shows that the complex was stable up to 246^{o}C. The first weight loss of 2.7% at 130^{o}C corresponds to the loss of coordinated H_2O molecules (expected, 5.3%). The next step represents a total weight loss of 87.4% and is assigned to the decomposition of the ligand (expected, 87%). The amount of residue at 875^{o}C is 9.6%. Assuming that the residue is NiO [Mehmet, TGA], the expected value is 10.4%, which is within the acceptable experimental error [73].

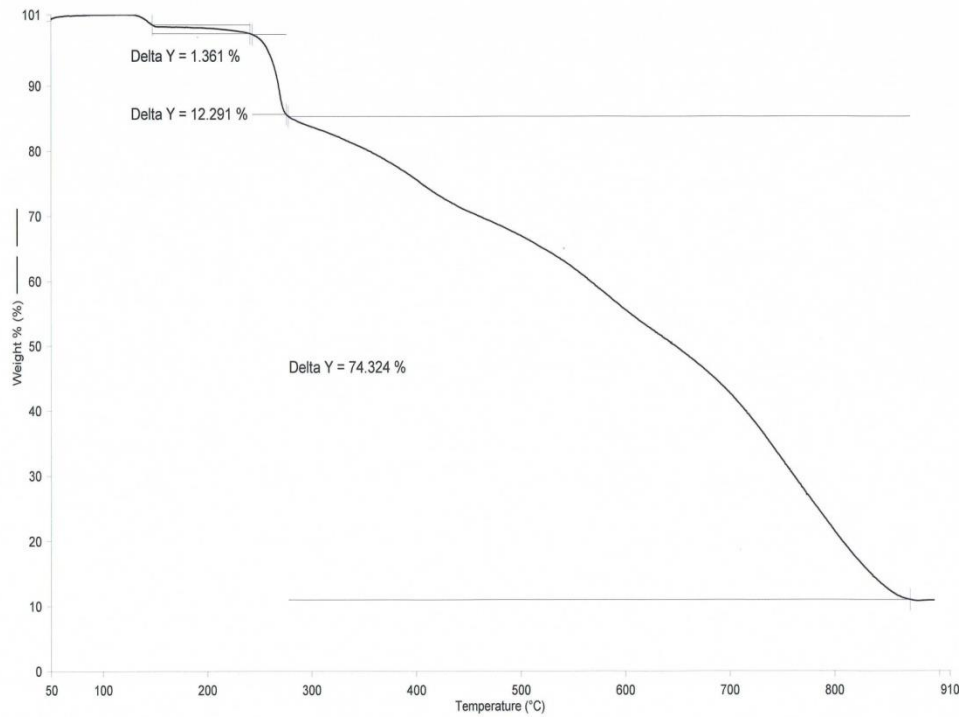

Figure 4.83TGA for [NiL6(H_2O)$_2$]

Based on the above analytical results, the proposed structure for [NiL6(H_2O)$_2$] is shown in **Figure 4.84.**

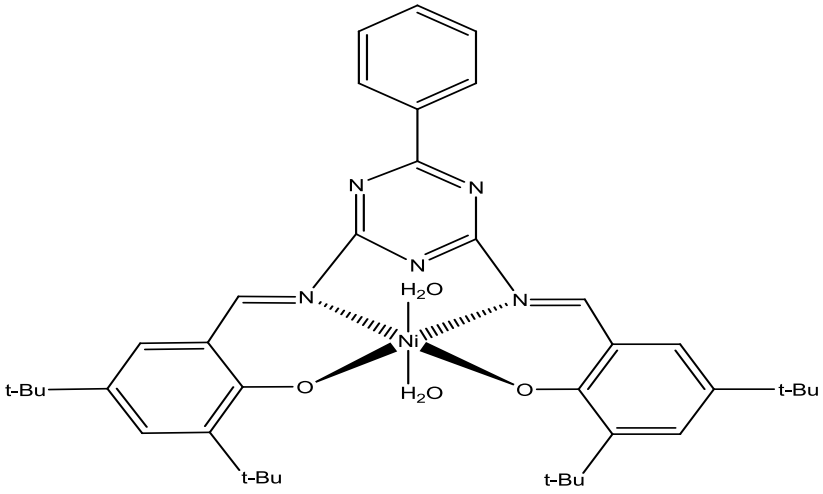

Figure 4.84 Proposed structural formula of [NiL6(H_2O)$_2$]

4.7.3 Copper(II) complex of H_2L6

The copper(II) complex was obtained as a dark green powder in good yield (78%) in the reaction between H_2L6 and copper(II) acetate monohydrate in presence of triethylamine. The yield is similar to Ni(II) complex (75%), indicating similar solubility in ethanol.

The results from the **CHN** elemental analyses are in excellent agreement with the expected chemical formula $CuC_{39}H_{47}O_2N_5$ or [CuL6 (H_2O)].

The **FTIR** spectrum (**Figure 4.85**) shows the expected functional groups as previously discussed for the corresponding Ni(II) complex (**Figure 4.81**). The C=N, C-O and Cu-O peaks for [CuL6].H_2O are at 1605 cm^{-1}, 1241 cm^{-1} and 546 respectively. These are almost similar to those of the corresponding Ni(II) complex, suggesting similar bond strength.

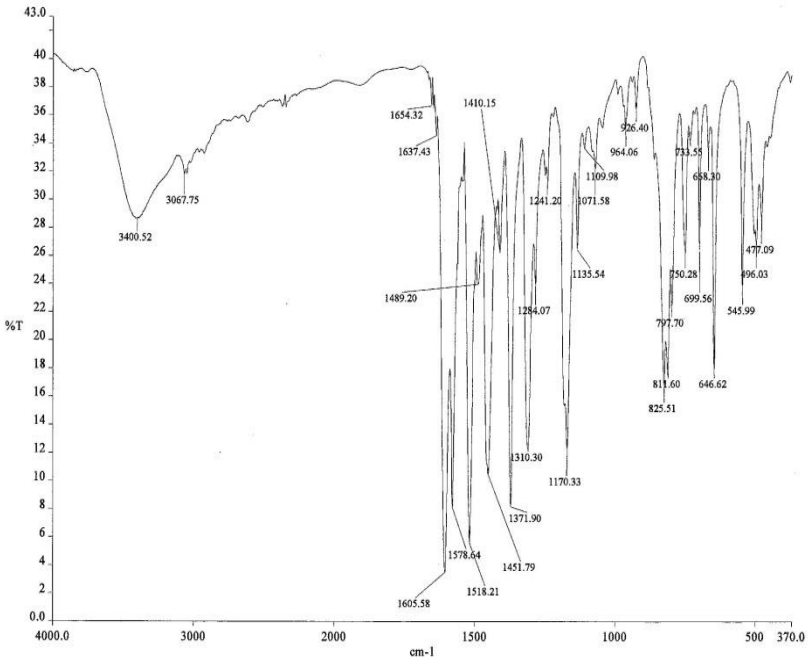

Figure 4.85 FTIR spectrum of [CuL6(H_2O)]

The **UV-vis** spectrum (**Figure 4.86**) shows a broad *d-d* peak at 670 nm (ε_{max} = 200 M^{-1} cm^{-1}). Thus, [CuL6(H_2O)] is a mononuclear square pyramidal complex [58]. The π - π^* and MLCT bands are at 297 nm (ε = 2.5 x 10^4 $M^{-1}cm^{-1}$) and 402 nm (ε = 1.02 x 10^4 $M^{-1}cm^{-1}$) respectively, which are almost the same as for the corresponding Ni(II) complex (274 nm, 410 nm), and may be similarly explained.

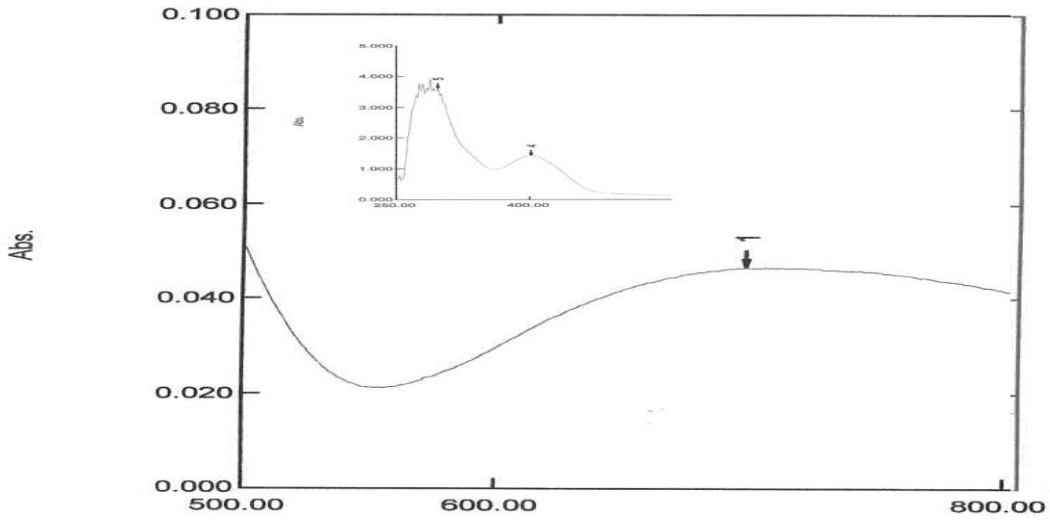

Figure 4.86 UV-vis spectrum of [CuL6(H_2O)]

The **TGA** thermogram **(Figure 4.87**), measured from 50^oC up to 900^oC, shows that the complex was stable up to 250^oC. Thus, it is as themally stable as [NiL6(H_2O)$_2$] (246^oC). The first weight loss of 3.5% at 140^oC corresponds to the loss of coordinated H_2O molecule (expected, 2.5%). The next step represents a total weight loss of 83.3% and is assigned to the decomposition of the ligand (expected, 88.6%). The amount of residue at about 650^oC is 13.2%. Assuming that the residue is CuO, the expected value is 11.1%. Thus, the thermal properties of [CuL6(H_2O)] is similar from that of [NiL6(H_2O)$_2$].

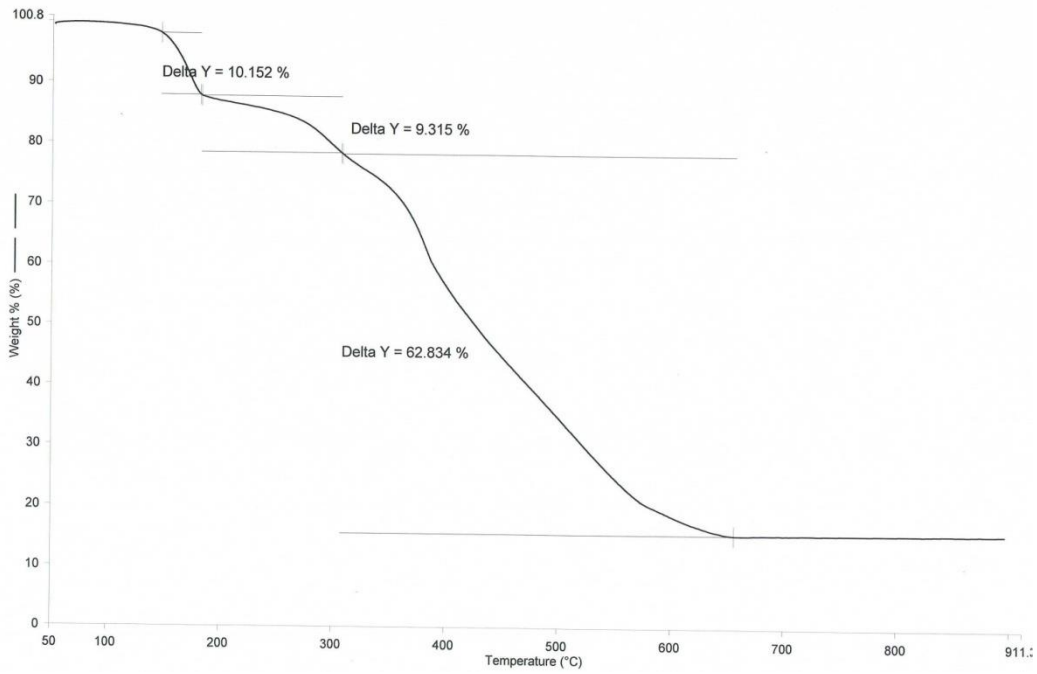

Figure 4.87 TGA for [CuL6(H_2O)]

Based on the above analytical results, the proposed structure for [CuL6(H_2O)] is shown in **Figure 4.88.**

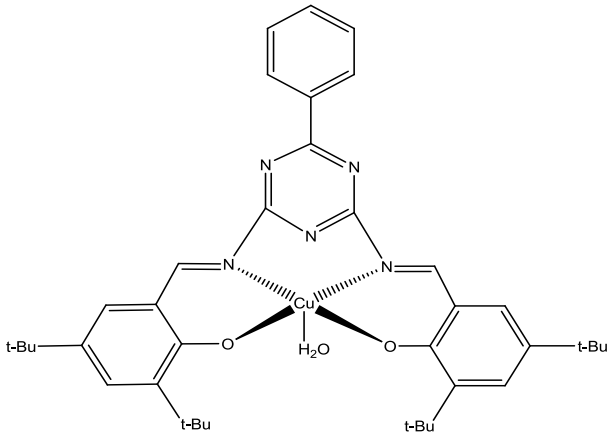

Figure 4.88 Proposed structural formula of [CuL6(H_2O)]

4.7.4 Zinc(II) complex of H_2L6

The zinc(II) complex was obtained as a light yellow powder in good yield (75%) in the reaction between $H_2L6$and zinc(II) acetate dihydrate in presence of triethylamine. The yield is similar to Cu(II) complex (78%) , indicating similar solubility in ethanol.

The results from the **CHN** elemental analyses are in excellent agreement with the expected chemical formula $ZnC_{39}H_{47}O_2N_5$ or $[ZnL6].2H_2O$.

The **FTIR** spectrum of $[ZnL6].2H_2O$ (**Figure 4.89**) shows the presence of all the expected functional groups. The wavenumbers of C=N (1608 cm^{-1}) and C-O (1240 cm^{-1}) groups are almost the same as for $[CuL6(H_2O)]$ (1605cm^{-1} and 1241 cm^{-1} respectively.

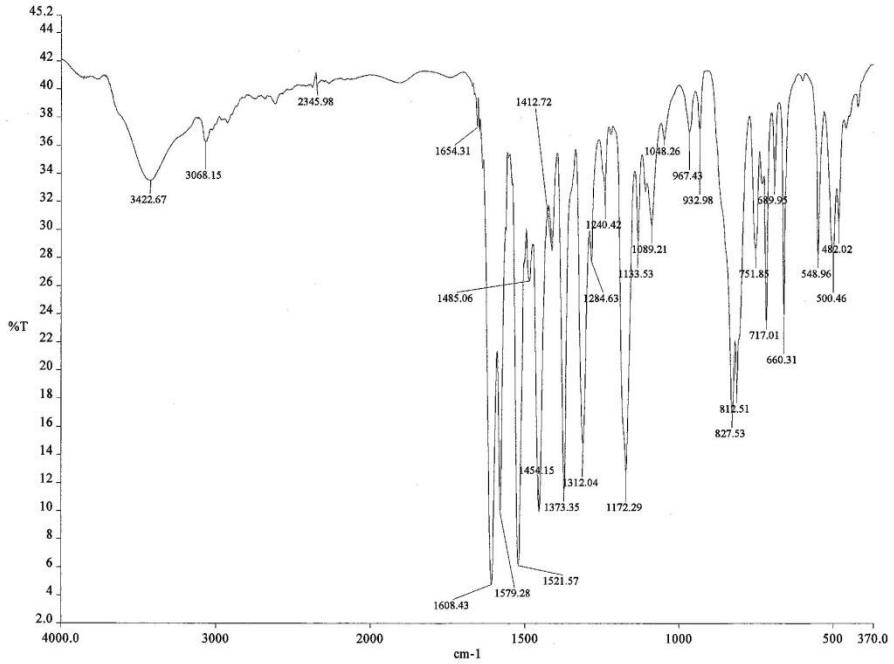

Figure 4.89 FTIR spectrum of $[ZnL6].2H_2O$

The **UV-vis** spectrum of [ZnL6].2H_2O (**Figure 4.90**) shows that the MLCT and π - π^*peaks 390 nm(ε = 1.7 x 10^4 $M^{-1}cm^{-1}$) and 275 nm(ε = 2.5 x 10^4 $M^{-1}cm^{-1}$) are at almost the same energy as the corresponding peaks for [CuL6 (H_2O)] (402 nm, 297 nm; **Figure 4.86**). Thus, both metal ions have insignificant effect on the electronic transitions of the organic moiety. The MLCT peak is normally observed from 348 nm to 323 nm for Zn(II) complexes, involving electronic transitions from the full *d* orbitals of the metal ion ($3d^{10}$) to antibonding orbitals of the ligand [75].

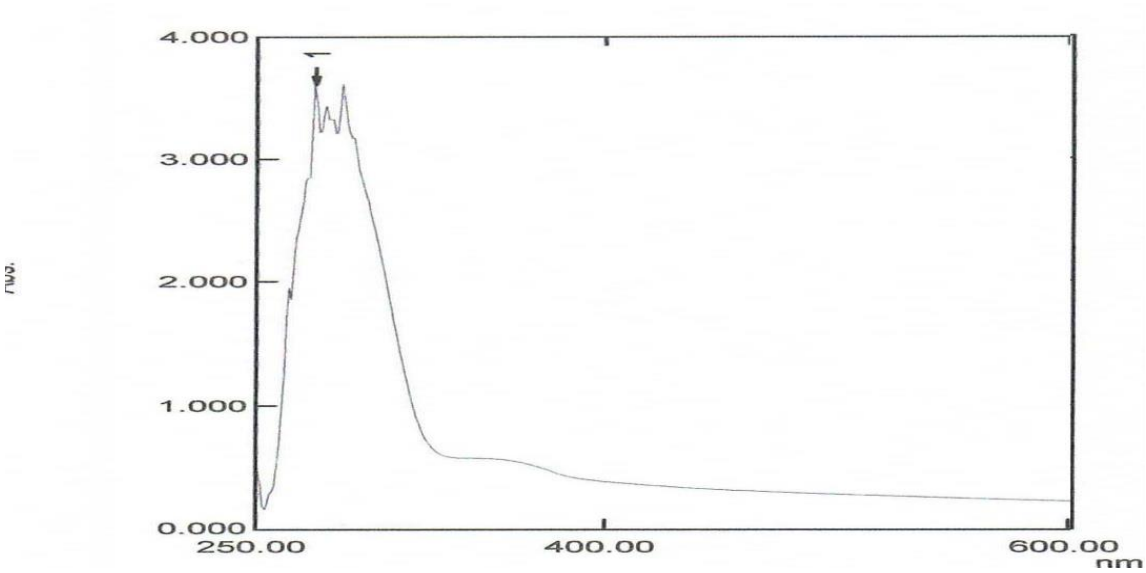

Figure 4.90 UV-vis spectrum of [ZnL6].2H_2O

The **TGA** thermogram **(Figure 4.91**), measured from 50^{o}C up to 900^{o}C, shows that the complex was stable up to 245^{o}C. Thus, it is as themally stable as [CuL6(H_2O)] (250^{o}C) and [NiL6(H_2O)$_2$] (246^{o}C). The results seem to suggest that the presence of different metal ions in the ligand has insignificant effect on the thermal stability of these complexes.

The first weight loss of 3.7% at 150^{o}C corresponds to the loss of coordinated H_2O molecules (expected, 5.1%). The next step represents a total weight loss of 86.1% and is assigned to the decomposition of the ligand (expected, 86.2%). The amount of residue at 850^{o}C is 10.2%. Assuming that the residue is ZnO, the expected value is 11.3%, which is within the acceptable experimental error.

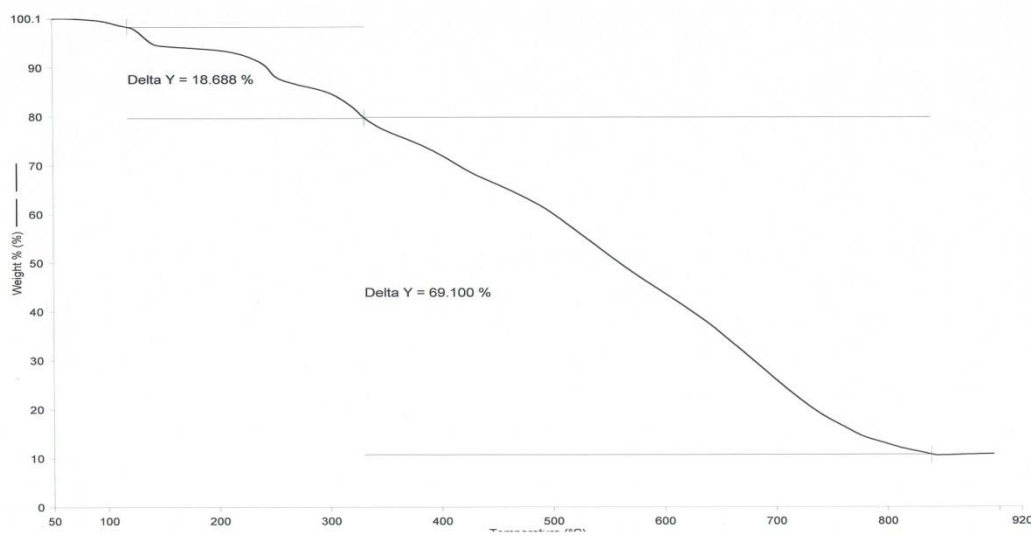

Figure 4.91 TGA for [ZnL6].2H_2O

Based on the above analytical results, and on the knowledge that Zn(II) prefers tetrahedral geometry, the proposed structure for [ZnL6].2H_2O is shown in **Figure 4.92.**

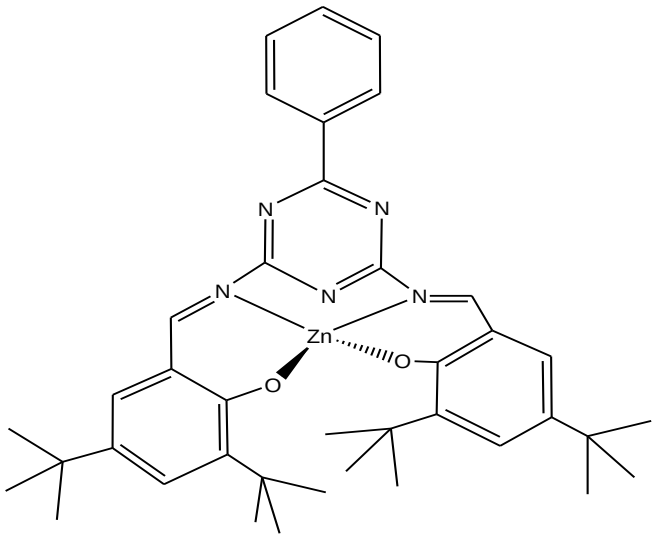

Figure 4.92 Proposed structural formula of [ZnL6].2H_2O (the solvate H_2O is not shown)